Characterizing the influence of Temperature on the short-term mechanical properties of 3D printed PLA

Jahidul Islam

Degree Thesis

Mechanical and Sustainable Engineering

2024

Degree Thesis

Jahidul Islam

Characterizing the influence of Temperature on the short-term mechanical properties of 3D printed PLA.

Arcada University of Applied Sciences: Mechanical and Sustainable Engineering, 2024.

Commissioned by:

Arcada University of Applied Sciences

Identification number:

047774771

Abstract:

This thesis investigates the influence of temperature on the mechanical properties of Polylactic Acid (PLA) manufactured using 3D printing, with a particular focus on tensile modulus and yield strength. The study adheres to the ISO 527 2/1B standard for developing tensile specimens, which were fabricated using a Creality Ender-3 Pro 3D printer employing Fused Deposition Modelling (FDM) technology. Specimens were printed with alternating orientations of (0°, 90°) and (45°, -45°) and at three different infill densities: 50%, 75%, and 100%. The mechanical properties were evaluated at four distinct temperatures: 20°C, 35°C, 40°C, and 50°C. The results demonstrated a clear trend of decreasing tensile modulus and yield strength with increasing temperature. As the temperature rose, the specimens became softer and lost both strength and stiffness. There are various limitations associated with using above glass transition temperature (≈60°C). In this case, PLA undergoes a transition to a more flexible state, which decreases its mechanical strength and makes it less indicative of normal usage conditions. This results in imprecise evaluations of its effectiveness. Additionally, a comparative analysis revealed that the (0°, 90°) infill orientation generally provided better load distribution and resistance than the (45°, -45°) infill orientation. This means that applied forces were more equally distributed and handled throughout the structure, leading to greater

resistance to deformation. Higher tensile modulus and yield strength at elevated temperatures were the result of this effective load control, which improved the material’s overall performance and resilience under stress. Finally, the mechanical constants were evaluated from modulus vs temperature & yield strength vs temperature graph. This study offers valuable insights for enhancing the design and application of PLA in environments subjected to varying thermal conditions, thereby improving reliability and performance. Future research may expand the range of temperature variations and investigate additional mechanical properties to achieve a more comprehensive understanding of PLA's behaviour under different conditions.

Keywords:

Additive Manufacturing, 3D printing, Fused Deposition Modelling, Infill Orientation, Infill Density, Polylactic acid.

List of Symbols

E	Tensile Modulus
ε	Tensile strain
σ	Tensile stress
R_e	Yield strength
F	Applied Force
A	Cross-sectional Area

Abbreviations

PLA	Polylactic Acid
AM	Additive Manufacturing
CAD	Computer Aided Design
IO	Infill Orientation
TM	Tensile Modulus
YS	Yield Strength
FDM	Fused Deposition Modelling
LAM	Lithographic Additive Manufacturing
LOM	Laminated Object Manufacturing
UAV	Ultrasound Additive Manufacturing
AI	Artificial Intelligence
ABS	Acrylonitrile Butadiene Styrene
PETG	Polyethylene Terephthalate Glycol
ML	Machine Learning
DIW	Direct Ink Writing
DLP	Digital Laser Processing
EBM	Electron Beam Melting
SLS	Selective Laser Sintering
SLM	Selective Laser Melting

Contents

1 INTRODUCTION

1.1 Background

Additive Manufacturing (AM), also known as three-dimensional (3D) printing, has revolutionized the manufacturing industry by offering significant cost reductions through minimized material waste and the ability to create complex geometries without traditional tooling (Foltut et al., 2023). Polymers, metals, ceramics, composites and even biomaterials can be utilised in the AM process. Specially, plastics play a crucial role in this process due to their advantageous properties, such as being lightweight, flexible, durable, chemically resistant, and inexpensive to produce. These characteristics make plastics indispensable in various engineering fields, including automotive, electrical, aerospace, construction, medical, and robotics sectors (Idumah & Nwuzor, 2019)

Most conventional plastics are derived from petroleum-based monomers like propylene and ethylene. While these plastics offer numerous benefits, their non-biodegradable nature poses significant environmental challenges (Geyer et al., 2017). In response to these issues, polylactic acid (PLA), a biodegradable polymer derived from renewable resources, has emerged as a sustainable alternative. PLA is widely used in numerous applications to replace petroleum-derived polymers, contributing to environmental sustainability efforts (Mustafa et al., 2021).

Understanding the impact of temperature on the mechanical properties of PLA is vital for enhancing the performance and reliability of 3D printed components in real-world applications. As the demand for sustainable and efficient manufacturing solutions grows, it is essential to comprehend how temperature variations affect the mechanical characteristics of PLA. This knowledge will aid in developing more reliable and high-performing 3D printed products, thereby advancing the fields of additive manufacturing and polymer science.

Previous research has extensively explored the mechanical properties of 3D printed PLA components, focusing on various factors such as infill density, infill pattern, and infill orientation. For instance, studies by (Ambati & Ambatipudi, 2022) and (Rana, 2022) investigated the influence of infill density and orientation on the mechanical properties of PLA

components. Similarly, (Tran, 2019) examined the impact of printing orientation on the tensile characteristics of FDM-produced components. (Gebrehiwot et al., 2020) observed how stiffener geometry affects 3D printed polylactic acid (PLA) beam flexural characteristics. (Gebrehiwot et al., 2023) also optimised the mechanical properties of additive-manufactured recycled polylactic acid (rPLA) utilising single and multi-response analysis. (Gebrehiwot et al., 2023) one more examined the short-term creep and recovery of injection-molded and additive-manufactured tough polylactic acid polymer. However, these studies did not specifically address the influence of temperature on the short-term mechanical properties of 3D printed PLA.

(Jayanth et al., 2021) conducted research on the impact of heat treatment on the mechanical characteristics of 3D printed PLA, while (Bakar et al., 2022) investigated the mechanical properties of PLA under different temperatures and environmental conditions. Although these studies provide valuable insights, they did not focus on a comprehensive analysis of the impact of 20°C, 35°C, 40°C and 50°C on the mechanical properties of 3D printed PLA. This thesis aims to fill this gap by examining the effects of four distinct temperature variations at different infill orientations and different infill densities on the tensile modulus and yield strength of 3D printed PLA components.

1.2 Objectives

The primary aim of this thesis is to analyse and describe how factors such as temperature, infill orientation, and infill density affect the mechanical properties of 3D printed PLA. Specifically, the study aims to investigate the general stress-strain relationship of the material at different temperatures. The tensile test specimens will be produced using FDM printing technology with different infill orientations (0°, 90°) & (45°, -45°) and three infill density percentages (50%, 75%, 100%). These specimens will be tested using the Testometric X350-20 machine at four different temperatures (20°C, 35°C, 40°C, & 50°C).

Upon acquiring all the data, the subsequent information will be elucidated in the discussion section:

- The influence of temperatures on the tensile modulus of PLA.
- The influence of temperatures on the yield strength of PLA.

The mechanical constants will be examined from the tensile modulus vs temperature and yield strength vs temperature curve.

The conclusion will summarize the impact of the four distinct temperatures on the tensile modulus and yield strength of PLA material.

1.3 Relevance to the Degrees Programme

This thesis is highly relevant to the Mechanical and Sustainable Engineering degree program, which emphasizes polymer design, 3D printing, mechanical testing, and data analysis. These components are integral to the study program, aligning with the goals of this research. From a mechanical engineering perspective, this thesis involves the examination and evaluation of various mechanical properties of PLA materials under different conditions, aiming to identify the most optimal configuration for additive manufacturing applications.

By integrating knowledge from polymer science, materials engineering, and mechanical testing, this research contributes to the development of sustainable and efficient manufacturing processes. The findings of this study will enhance the understanding of how temperature variations influence the mechanical properties of 3D printed PLA, providing valuable insights for future research and industrial applications.

In conclusion, this thesis aims to bridge the knowledge gap regarding the impact of temperature on the mechanical properties of 3D printed PLA. By investigating the tensile modulus and yield strength of PLA under various temperature conditions, this research will provide a comprehensive understanding of the factors influencing the performance of 3D printed components. The outcomes of this study will contribute to the advancement of additive manufacturing technologies and support the development of more reliable and high-performing 3D printed products.

2 LITERATURE REVIEW

2.1 Evolution of 3D Printing

The evolution of 3D printing, also known as additive manufacturing, has been marked by significant technological advancements and growing applications across various industries. This section explores the historical development of 3D printing, highlighting key milestones and technological innovations that have shaped its current state. The concept of 3D printing can be traced back to the early 1980s. The first significant milestone was the invention of stereolithography (SLA) by Charles Hull in 1983 (Hull, 1983). Hull's innovation involved curing liquid photopolymer resin layer by layer using ultraviolet (UV) light, allowing the creation of complex three-dimensional objects directly from digital models. Hull's work laid the foundation for the development of other 3D printing technologies and led to the establishment of 3D Systems, a company that played a pivotal role in commercializing 3D printing technology.

In 1988, Carl Deckard at the University of Texas developed Selective Laser Sintering (SLS), which used a laser to fuse powdered materials into solid structures. This technology broadened the range of materials that could be used in 3D printing, including metals and ceramics, significantly expanding the potential applications of additive manufacturing (Das et al., 2023). The 1990s saw further advancements and diversification of 3D printing technologies. Fused Deposition Modelling (FDM), developed by Scott Crump and commercialized by Stratasys, became one of the most popular and widely used 3D printing methods. FDM works by extruding thermoplastic filaments through a heated nozzle, building objects layer by layer. Its affordability and ease of use made it accessible to a broader range of users, including hobbyists and educational institutions (Das et al., 2023).

Another notable development during this period was the introduction of Lithographic additive Manufacturing (LAM). Photopolymers have become the most popular AM materials during the last thirty years because LAM technologies find wide uses in the aerospace, automotive,

healthcare, biomedical, furniture, fashion, and entertainment sectors (Melentiev et al., 2024). Two more remarkable processes are laminated object manufacturing (LOM) and ultrasound additive manufacturing (UAM). The benefits of this method include the ability to produce full-color prints, its cost-effectiveness, ease of material handling, and the ability to recycle extra material. Complicated geometrical pieces can be produced by LOM at a reduced fabrication cost and shorter operation time. UAM is a cutting-edge industrial method that utilizes sound waves to combine layers of metal extracted from plain foil material (Shahrubudin et al., 2019)

While consumer 3D printing gained popularity, industrial applications of additive manufacturing continued to grow. The aerospace, automotive, and healthcare industries recognized the potential of 3D printing for producing complex, lightweight, and customized components. In the aerospace industry, companies like Boeing and Airbus adopted 3D printing to manufacture parts for aircraft, taking advantage of the technology's ability to reduce weight and material waste. The automotive industry also explored 3D printing for rapid prototyping, tooling, and even end-use parts. For example, Ford used 3D printing to produce prototypes and custom tools, significantly reducing development time and costs. The healthcare sector also witnessed groundbreaking applications of 3D printing in the production of custom implants, prosthetics, and medical devices. Bioprinting, which involves printing with bio-inks composed of living cells, emerged as a promising field with the potential to create tissue and organ constructs for regenerative medicine and transplantation (Saini et al., 2021 & Yankin et al., 2023).

In recent years, 3D printing has continued to evolve, driven by advancements in technology and materials. Multi-material and multi-color printing capabilities have enabled the creation of more complex and aesthetically appealing objects. Additionally, improvements in speed and precision have made additive manufacturing more competitive with traditional manufacturing methods. The integration of artificial intelligence (AI) and machine learning (ML) into 3D printing workflows has also shown promise in optimizing print quality, reducing defects, and enhancing process efficiency (Goh & Yeong, 2022).

Looking ahead, the future of 3D printing holds exciting possibilities. The continued development of new materials, including advanced polymers, composites, and biocompatible materials, will further expand the range of applications. Large-scale 3D printing, such as

construction printing, has the potential to revolutionize the construction industry by enabling the rapid and cost-effective production of buildings and infrastructure.

2.2 Role of Thermoplastic Polymers

Thermoplastic polymers play a crucial role in 3D printing due to their ability to soften when heated and harden upon cooling, making them ideal for various additive manufacturing processes. These materials, including PLA (Polylactic Acid), ABS (Acrylonitrile Butadiene Styrene), PETG (Polyethylene Terephthalate Glycol), and Nylon, offer versatility, durability, and ease of processing. In Fused Deposition Modeling (FDM), the most common 3D printing technique, thermoplastic filaments are extruded through a heated nozzle to build objects layer by layer. Their reusability and wide range of mechanical properties, from flexible to rigid, make thermoplastic polymers suitable for prototyping, functional parts, and consumer products, contributing to the broad adoption and continuous innovation in 3D printing technologies (Yankin et al., 2023).

2.2.1 Advantages of PLA in 3D Printing

Polylactic Acid (PLA) is one of the most popular thermoplastic polymers used in 3D printing due to its numerous advantages. PLA is aliphatic polyester which is derived from renewable resources like corn starch or sugarcane, making it an environmentally friendly alternative to petroleum-based plastics.

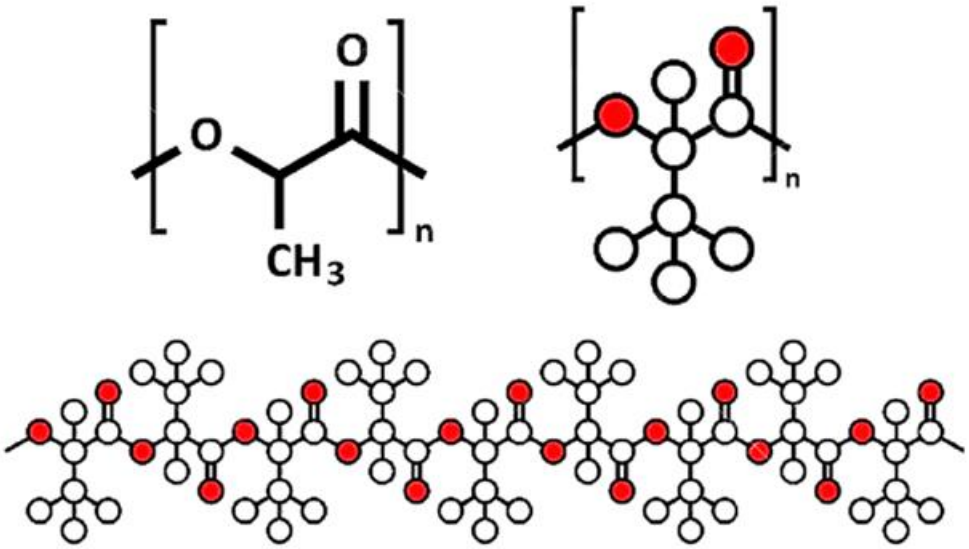

Figure 1. Chemical structure of polylactic acid

The biodegradable nature of PLA reduces the ecological footprint of 3D printing processes, aligning with growing environmental concerns and sustainability goals (Winter et al., 2023). PLA offers excellent printability, which makes it ideal for beginners and for creating high-resolution prints. It has a relatively low melting point, typically around 180-220°C, which means it can be processed using standard 3D printers without requiring specialized equipment (Hasan et al., 2024). The low melting temperature also contributes to energy efficiency during the printing process. The polymer's ability to produce fine details and smooth surfaces is another significant advantage. PLA printed objects exhibit minimal warping and shrinkage, which are common issues with other thermoplastics like ABS. This stability during the printing process ensures high accuracy and consistency in the printed parts (Joseph et al., 2023).

Moreover, PLA exhibits good mechanical properties for many applications. It provides sufficient strength and rigidity for a variety of uses, including prototypes, educational models, and consumer products. While it may not be as strong as some engineering plastics, its mechanical properties are adequate for many non-structural applications. In addition to these practical advantages, PLA is available in a wide range of colors and can be combined with other materials, such as carbon fiber, to enhance its properties. Carbon fiber-reinforced PLA composites are increasingly used to create parts with improved strength and stiffness while maintaining the ease of processing associated with PLA (Maqsood & Rimašauskas, 2021).

2.3 Printing Techniques

3D printing, or additive manufacturing, has revolutionized the manufacturing industry by enabling the production of complex geometries and custom parts with unprecedented precision and efficiency. Various printing techniques have been developed over the years, each offering unique advantages and suitable for different applications. This section provides a detailed literature review on the most prominent 3D printing techniques, including Fused Deposition Modeling (FDM), Direct Ink Writing (DIW), and other advanced methods (Baniasadi et al., 2024 & Das et al., 2023).

2.3.1 Fused Deposition Model (FDM)

FDM is one of the most widely used 3D printing techniques, known for its simplicity, cost-effectiveness, and versatility. In FDM, thermoplastic filaments are heated to their melting point and extruded through a nozzle to build objects layer by layer. The process starts with the creation of a digital model, which is sliced into thin layers by the printer's software. The nozzle moves in the X and Y directions to deposit the melted filament, and the build platform lowers gradually to add successive layers. FDM is compatible with various thermoplastics, including PLA, ABS, PETG, and more advanced composites like carbon fiber-reinforced polymers. Its advantages include ease of use, minimal material waste, and the ability to produce functional prototypes and end-use parts. However, FDM also has limitations, such as lower resolution compared to other techniques and potential issues with layer adhesion and warping. Recent advancements in FDM technology focus on improving print quality, speed, and expanding the range of printable materials, making it a continually evolving and vital part of the 3D printing landscape (Chhabra, 2017).

2.3.2 Direct Ink Writing (DIW)

Direct Ink Writing (DIW) is an advanced additive manufacturing technique that involves the precise extrusion of viscoelastic inks through a fine nozzle to create intricate structures layer by layer. This method is highly versatile, accommodating a wide range of materials, including polymers, ceramics, metals, and composite inks. DIW is particularly beneficial for applications requiring customized material properties and complex geometries, such as biomedical devices, electronics, and structural components. The process starts with preparing an ink that has suitable rheological properties, ensuring it flows easily through the nozzle but maintains its shape upon deposition. DIW allows for the inclusion of functional materials, such as conductive inks, bioinks, and magnetically responsive materials, enabling the fabrication of multi-material and multi-functional devices. One of the key advantages of DIW is its ability to print at room temperature, making it ideal for materials sensitive to high temperatures. Additionally, DIW can achieve high-resolution prints with fine feature details, suitable for both prototyping and production. However, the process requires careful formulation and optimization of inks to ensure consistent quality and performance. As research progresses, DIW continues to expand its capabilities, offering new possibilities for advanced manufacturing and material innovation (Antanitta S et al., 2024 & Baniasadi et al., 2024).

2.3.3 Other Techniques

Beyond FDM and DIW, the landscape of 3D printing encompasses a diverse array of techniques, each suited to specific applications and material requirements. Stereolithography (SLA) and Digital Light Processing (DLP) are resin-based methods known for their high resolution and smooth surface finishes. In SLA, a laser cures liquid resin layer by layer, while DLP uses a digital light projector to flash entire layers at once, speeding up the process. Both techniques are ideal for detailed prototypes, dental models, and jewelry. Selective Laser Sintering (SLS) and Selective Laser Melting (SLM) use lasers to sinter or melt powdered materials, typically polymers or metals, to create robust and intricate parts. These methods are particularly valuable in aerospace and medical industries, where complex geometries and high-performance materials are essential. Binder Jetting and Material Jetting are other noteworthy

techniques; Binder Jetting deposits a binding agent onto a powder bed to form parts, while Material Jetting sprays droplets of material, which are then cured or solidified. Both methods offer multi-material and full-colour printing capabilities. Additionally, techniques like Electron Beam Melting (EBM) and Laminated Object Manufacturing (LOM) cater to specific industrial needs, such as high-density metal parts and layered construction of sheet materials. Each of these techniques presents unique benefits and challenges, contributing to the expansive and rapidly evolving field of additive manufacturing (Chhabra, 2017).

2.4 Mechanical Properties of PLA

The mechanical properties of PLA make it an attractive option for a wide range of applications, from prototyping to manufacturing functional parts. This scientific passage explores the mechanical properties of PLA in 3D printing, covering aspects such as tensile strength, Young's modulus, elongation at break, impact resistance, and factors that influence these properties, including print parameters and post-processing treatments.

The tensile modulus, also known as Young's modulus, is a fundamental mechanical property that measures a material's stiffness and elasticity. It is defined as the ratio of tensile stress (force per unit area) to tensile strain (proportional deformation) in the linear elastic region of the material's stress-strain curve. The tensile modulus is expressed in units of pressure, typically pascals (Pa) or megapascals (MPa) and is a critical parameter in engineering and materials science (Grant & Phillips, 2001, pp. 510-512). In the context of 3D printing, the tensile modulus provides valuable insights into the quality and performance of printed parts, influencing their structural integrity, durability, and suitability for various applications.

Tensile stress is computed by dividing parallel force components by their area. Its unit is Pascal (Pa). The tensile stress (σ) can be mathematically expressed using the formula:

$$\sigma = \text{Force} / \text{Cross-sectional area} = F/A \quad \text{.....(1)}$$

On the other hand, tensile strain may be determined by dividing the amount of deformation in the direction of the applied force by the material's original length. It has no unit.

$$\varepsilon = \text{Change in length/original length} = \Delta L/L_0 \qquad (2)$$

Therefore, according to the SFS-EN ISO 527-1:2019:en the tensile modulus (E) can be mathematically expressed as chord slope using the formula:

$$E_t = (\sigma_2 - \sigma_1) / (\varepsilon_2 - \varepsilon_1) \qquad (3)$$

Where:

E_t is the tensile modulus

σ_1 is the stress, measured at the strain value ε_1

σ_2 is the stress, measured at the strain value ε_2

2.4.1 Factors Affecting to the Tensile Modulus

In 3D printing, the tensile modulus of printed parts can be influenced by various factors, including the type of material used, printing parameters, and the geometry of the print. For instance, thermoplastic polymers like PLA, ABS, and PETG each have distinct tensile moduli, which can be further modified by the printing process. The layer-by-layer deposition method intrinsic to 3D printing can introduce anisotropies in mechanical properties, meaning that the tensile modulus may vary depending on the direction of the applied load relative to the printed layers. This anisotropy must be carefully managed to ensure the overall performance and reliability of the printed part (Kharat et al., 2023 & Algarni & Ghazali, 2021).

2.4.1.1 Material Type

Different materials exhibit varying tensile moduli, which is a primary consideration in selecting materials for specific applications. Polymers, metals, and composites are commonly used in 3D printing, each offering distinct mechanical properties. For example, PLA typically has a tensile modulus around 3.5 GPa, while ABS is lower, around 2 GPa (Rajpurohit & Dave, 2018, Hasan et al., 2024 & Cantrell et al., 2016). Advanced composites, such as carbon fibre-reinforced PLA, can have significantly higher moduli due to the stiffening effect of the fibres. The choice of material thus directly impacts the tensile modulus and the performance of the printed part (Ferreria et al., 2017 & Turkea et al., 2024).

2.4.2 Printing Parameters

Printing parameters, including layer height, infill density, printing speed, and temperature, significantly affect the tensile modulus of 3D printed parts.

2.4.2.1 Layer Height

The layer height is a crucial parameter in 3D printing that directly impacts the printing process's quality, speed, and efficiency. Layer height is the parameter that specifies the thickness of each individual layer that is added to construct the final 3D object (Baniasadi et al., 2024). Thinner layers typically result in better interlayer adhesion, leading to higher tensile modulus values. Thicker layers may produce parts with lower stiffness due to weaker bonding between layers (Ahmad & Yahya, 2023).

2.4.2.2 Infill Density

Infill density determines the amount of material used within the interior of a 3D printed part, expressed as a percentage of the total volume. Higher infill densities result in stronger and more rigid parts but also increase material usage and printing time. Conversely, lower infill densities reduce material consumption and weight but can compromise the mechanical integrity of the part (Naik et al., 2022 & Turaka et al., 2024). Infill density is a critical parameter for balancing strength, weight, and cost in 3D printing with PLA. For structural applications, infill densities of 50% or higher are often recommended, while for non-structural or decorative parts, infill densities as low as 10-20% may suffice (Algarni & Ghazali, 2021). The choice of infill density should align with the specific requirements of the printed object, considering factors such as load-bearing capacity and intended use. The study conducted by (Abeykoon et al., 2020) demonstrated the relationship between the tensile modulus and infill density for pure PLA material. Specimens with infill density from 25% to 100% were tested. The results showed a positive correlation between infill density and tensile modulus, with higher infill densities leading to increased stiffness. The highest tensile modulus was observed in parts with 100% infill density, highlighting the importance of infill optimization for achieving desired mechanical properties.

2.4.2.3 Infill Orientation

The infill orientation plays a crucial role in determining the tensile modulus, which is a measure of the material's stiffness and its ability to resist deformation under tensile loads. Infill orientation refers to the direction and pattern in which the internal structure of a 3D printed part is deposited. Different infill orientations can significantly affect the mechanical properties of the printed part due to the anisotropic nature of the 3D printing process, where the mechanical properties can vary depending on the direction of the applied load relative to the

printed layers. Research has shown that aligning the infill pattern parallel to the direction of the applied load generally results in higher tensile modulus values. This is because the load is distributed more effectively along the continuous filament paths, which enhances the part's ability to resist deformation (Naik et al., 2022).

Numerous experimental studies have been conducted to quantify the impact of infill orientation on the tensile modulus of 3D printed parts. For instance, a study by (Ganeshkumar et al., 2022) involved printing PLA specimens with different infill orientations and testing them under tensile loads. The results showed a clear correlation between infill orientation and tensile modulus, with the highest modulus observed in specimens where the infill lines were aligned with the load direction. Similar findings were reported by (Yankin et al., 2023), who experimented with ABS and Nylon materials and found that optimizing infill orientation could enhance the tensile modulus.

Another study by (Calles et al., 2021) explored the effects of infill orientation on composite materials, such as carbon fiber-reinforced PLA. They observed that the tensile modulus could be significantly improved by aligning the carbon fibers with the load direction, demonstrating the critical role of infill orientation in composite 3D printing. These findings underscore the importance of considering infill orientation during the design phase to maximize the mechanical performance of 3D printed parts.

Theoretical models have also been developed to predict the impact of infill orientation on tensile modulus. These models consider the geometry of the infill pattern, the material properties, and the loading conditions. For example, Gibson and Ashby's cellular solids theory has been adapted to model the mechanical behaviour of 3D printed infill structures. This theory provides a framework for understanding how the infill pattern and infill orientation influence the overall stiffness and strength of the printed part (Zhong et al., 2023). Understanding the impact of infill orientation on tensile modulus has significant practical implications. For engineers and designers, optimizing infill orientation can lead to stronger, stiffer parts that perform better under load. This is particularly important in applications such as aerospace, automotive, and biomedical engineering, where mechanical performance is critical. Moreover, optimizing infill orientation can also lead to material savings and reduced print times, as it allows for the use of lower infill densities without compromising mechanical integrity.

2.4.2.4 Temperature

Printing temperature significantly affects the material behaviour during the 3D printing process. For thermoplastics, which are commonly used in FDM, the printing temperature must be high enough to melt the filament but not so high as to cause thermal degradation. Optimal temperature settings ensure that the material flows smoothly through the nozzle and adheres properly to the previous layer. For example, PLA typically requires a printing temperature between 180-220°C, while ABS needs a higher range of 220-250°C. Studies have shown that printing at temperatures too low can lead to issues such as under-extrusion, poor layer adhesion, and brittle parts (Algarni & Ghazali, 2021). Conversely, excessively high temperatures can cause filament oozing, warping, and a decrease in the mechanical strength of the printed part due to thermal degradation of the polymer chains (Hadi et al., 2023).

Besides the nozzle temperature, ambient temperature and cooling rates during and after printing also play crucial roles in determining the quality of 3D printed parts. The ambient temperature around the printer affects the cooling rate of the printed layers, which in turn impacts layer adhesion and warping. For instance, printing in a cooler environment can cause rapid cooling and shrinkage, leading to warping and poor layer adhesion. Conversely, a controlled ambient temperature helps in maintaining a uniform cooling rate, reducing the likelihood of defects. Active cooling mechanisms, such as fans and enclosures, are used to manage the cooling process. Research indicates that controlled cooling, combined with optimal printing temperatures, enhances the dimensional accuracy and mechanical properties of the printed parts by minimizing thermal stresses and warping (Pank et al., 2022, Jayanth et al., 2021 & Hadi et al., 2023).

2.4.2.5 Post-processing Techniques

Post-processing techniques, such as annealing, can further influence the effects of printing temperature on the mechanical properties of 3D printed parts. Annealing involves heating the

printed part to a specific temperature and then cooling it gradually to relieve internal stresses and enhance the material's crystalline structure. For instance, annealing PLA parts printed at optimal temperatures can increase their tensile strength and stiffness by promoting greater crystallinity and eliminating residual stresses. Studies have shown that annealed parts exhibit improved mechanical performance and dimensional stability compared to non-annealed parts, highlighting the significance of post-processing in conjunction with printing temperature optimization (Guduru & Srinivasu, 2020)

2.5 Yield Strength

According to the ISO 527, The strength of the yield, (Re) stands for the stress at which a material can undergo elastic deformation during a tensile test. The yield strength is expressed in N/mm^2 or MPa (Megapascal).

It is influenced by a multitude of factors such as, material properties, printing parameters and post-processing techniques. Temperature for example, affects the viscosity and flow behaviour of the material during printing, influencing the degree of interlayer bonding and the homogeneity of the printed part. Understanding these factors is therefore crucial for optimizing the mechanical properties and ensuring the structural integrity of 3D printed parts.

3 METHOD

3.1 Specimen Design

A popular 3D computer-aided design (CAD) software is highly valuable for achieving precise production of mechanical or manufacturing components. It is widely used in the design process to create new and innovative items. The tensile test specimen utilized in this thesis is constructed in SolidWorks based on the specified dimensions mentioned in the ISO 527-2/1B standard. The design dimensions of the specimen are illustrated in figure 2 and presented in table 1 below:

Table 1 Dimensions of the Tensile Test Specimen

Types of dimensions	**Values (mm)**
l_3	150
l_1	60
r	60
l_2	107.96
b_2	20
b_1	10
h (thickness)	4
Extruded out	4

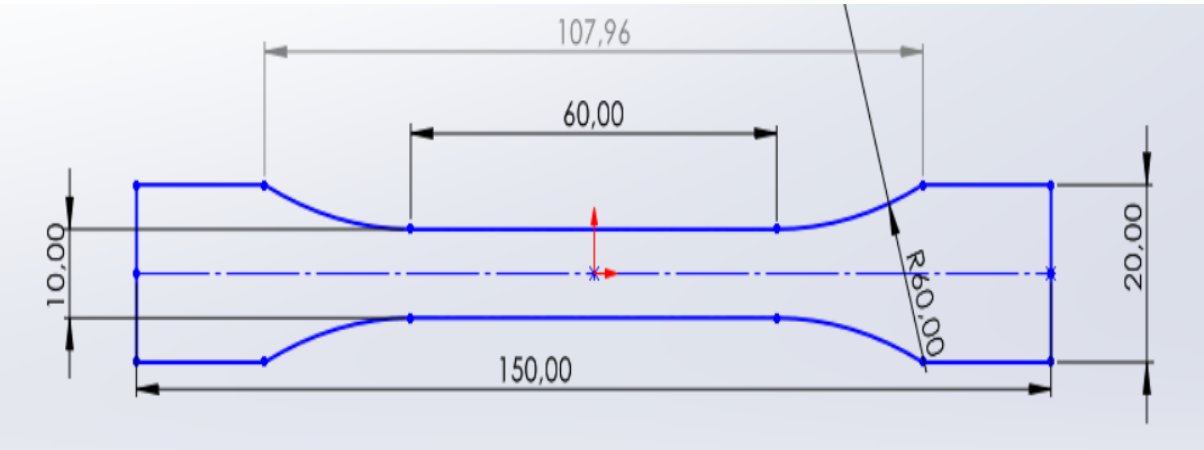

Figure 2. Specimen Dimensions

Figure 3 displays the finished specimen in its final image.

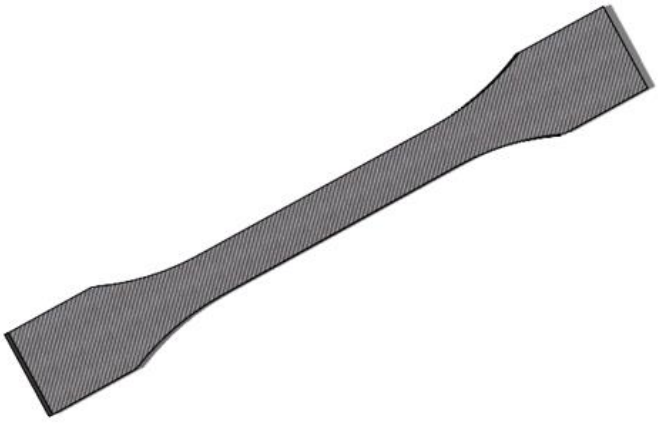

Figure 3. Designed Specimen

3.2 Specimen Print Settings

In this study, specimens were printed with two types of infill orientations (0°, 90°), (45°, -45°) and three different percentages of infill densities (50%, 75% and 100%). The default parameters of Cura software were used to ensure standard quality. Each specimen had a total thickness of 4 mm, with the top and bottom layers each measuring 0.4 mm and individual layers measuring 0.2 mm. This setup resulted in a 3.2 mm infill with different orientations. The print parameters are specified in Table 2.

Table 2 print settings

Print Settings	**Values**
Layer Height	0.2 mm
Top Bottom Thickness	0.4 mm
Top Thickness	0.4 mm
Top Layers	2
Bottom Thickness	0.4 mm
Bottom Layers	2
Infill Densities	50%, 75% and 100%
Infill Pattern	Lines
Infill Line Directions	[0°, 90°] and [45°, -45°]
Printing Temperature	215°C
Build Plate Temperature	70°C
Print Speed	150 mm/s

The specimens were created using a 3D printer with (0°,90°) and (45°, -45°) infill orientations. Infill orientations affect mechanical qualities and are crucial to additive manufacturing tensile test specimens. Different infill orientations impact material strength, stiffness, and failure. The best infill orientation increases load distribution and structural robustness, ensuring accurate test results. Tensile modulus is higher in (0°, 90°) infill patterns than (45°, -45°) (Chacón et al., 2017).

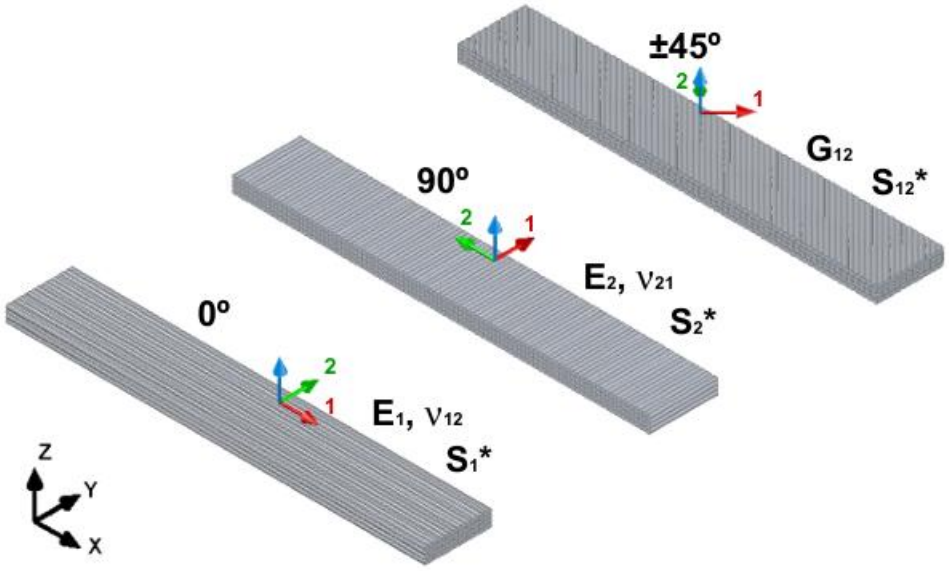

*Figure 4. Illustration of printing orientations (0°, 90° and 45°, -45°). The local material directions are 1, the direction of printing, and 2, perpendicular to 1. The global coordinates are x, y, z. (*Ferreira et al., 2017*)*

3.3 Slicing via Cura Software

After designing the part in CAD software, it can be converted into a tangible object through additive manufacturing. This process involves intermediate software such as Ultimaker Cura, which was used in this experiment. The CAD file was saved in STL format and imported into Cura, which slices the object into layers and generates a G-code—a set of instructions that the 3D printer can interpret. The G-code file was then transmitted to the 3D printer, initiating the sequential printing of the component according to the instructions in the G-code.

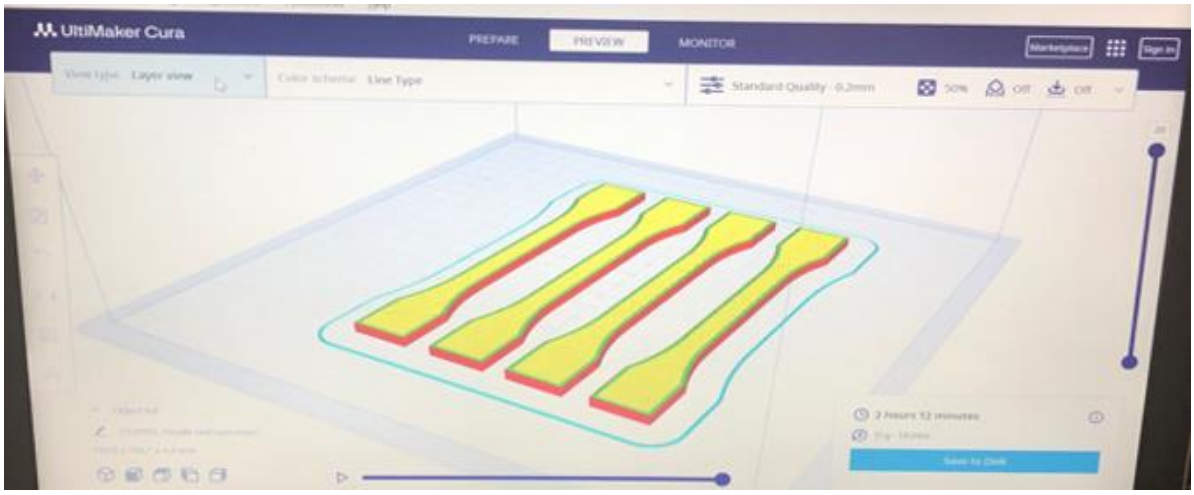

Figure 5. Sliced Specimen in Ultimaker Cura Software

3.4 3D Printer used in Printing Process

Figure 6 shows a picture of the printing tensile test specimens, and table 3 displays the printer's properties (*Ender-3 Pro 3D Printer).*

Figure 6. Tensile Test Specimens in Creality Ender-3 Pro 3D Printer

Table 3 Printer properties

Printer Parameters	**Values**
Machine Model	Ender-3 Pro
Molding Technology	FDM(Fused Deposition Molding)
Printing Size	220*220*250 mm
Printing Speed	≤180 mm/s, normal 30-60 mm/s
Printing Precision	±0.1mm
Nozzle Temperature	Standard 0.4 mm, can be in 0.3 or 0.2 mm
Hotbed Temperature	≤100°C
File Format	STL, OBJ, AMF
Slicing Software	Cura/Repetier-Host/Simplify3D
Filament	PLA, ABS, TPU, Wood, Copper etc.
Net Weight	6.98 Kg
Machine Size	440*420*465 mm

Figure 7. Printed Specimens at different densities and infill orientation (0°, 90°)

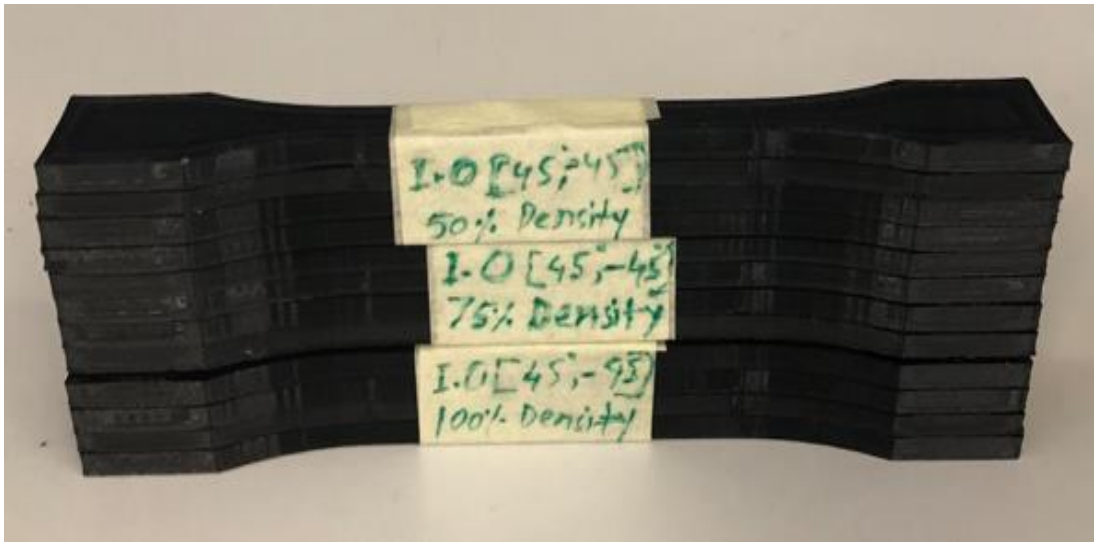

Figure 8. Printed Specimen at different densities and infill orientation (45°, -45°)

3.5 Temperature Control Device

A temperature controller from the E5AC series provides great visibility, a straightforward installation process, and precise control performance. A high-quality LCD display is included in this device, which is also very user-friendly and compact. Assuring accurate and responsive control is the rapid sample time of fifty milliseconds. Omron's 2-PID control algorithm contributes greatly to the enhancement of performance. When it comes to applications that are not as demanding, the controllers also provide simple on-off control (Omron automation E5AC). This device was operated by the TK Software.

Figure 9. Temperature Control Device

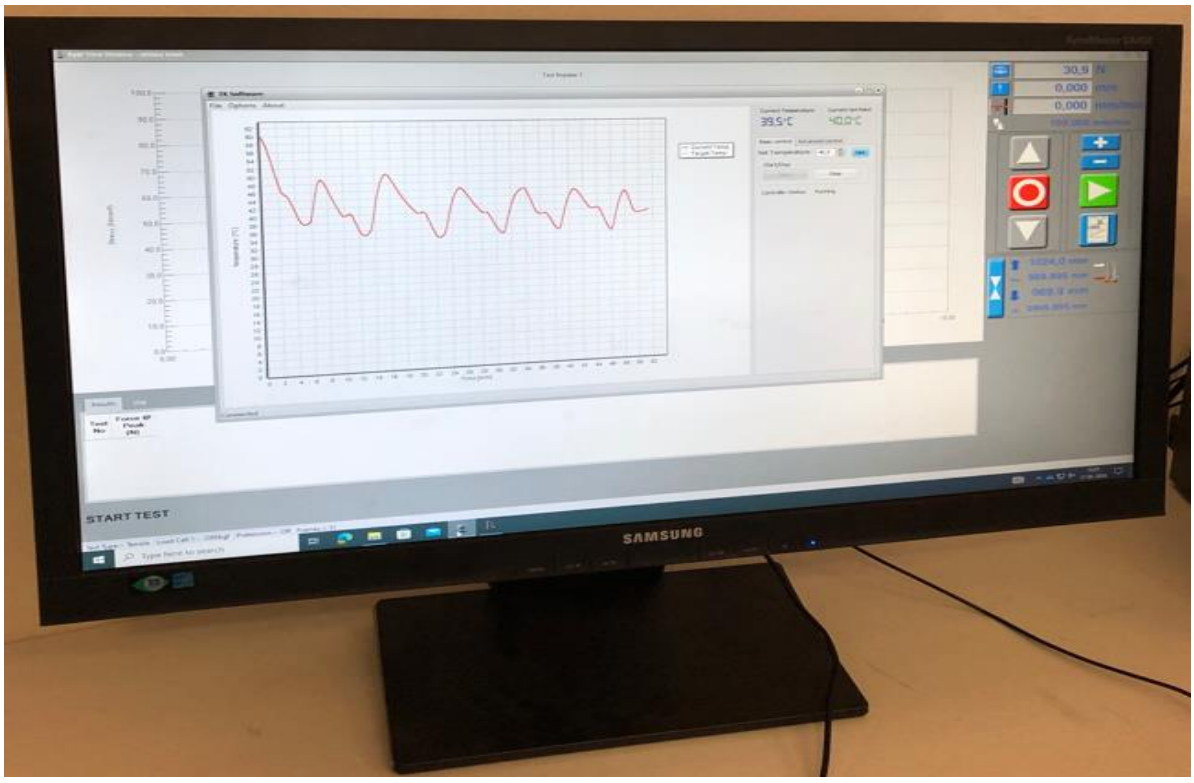

Figure 10. The TK Software

3.6 Tensile Modulus Testing

A highly advanced universal testing equipment, the Testometric X350-20 was developed for use in a wide variety of material testing including tensile, compression, and flexural tests. It has a maximum load capacity of 20 kN, which ensures that it is suitable for a wide range of materials, including metals and polymers. In addition to this, it has capabilities for detailed data analysis and reporting, which makes it an extremely useful instrument for research laboratories and quality control departments (AZO MATERIALS). A device known as the AMPROBE TMD-56 was used to measure the temperature of the sample.

Figure 11. Tensile modulus testing machine- Testometric X350-20 and AMPROBE TMD-56

4 RESULTS

4.1 Samples After Testing

The figure below illustrates the results of the tensile modulus testing conducted on PLA tensile test specimens using the Testometric X350-20 machine. The specimens were tested at various temperatures (20°C, 35°C, 40°C & 50°C) and infill orientations (0°, 90°) with a infill density of 50%.

Figure 12. Specimens after tensile modulus testing

The diagram below depicts the outcomes of the tensile modulus testing carried out on PLA tensile test specimens with the Testometric X350-20 equipment. The specimens underwent testing at different temperatures (20°C, 35°C, 40°C & 50°C) and infill orientations (0°, 90°) while maintaining a infill density of 75%.

Figure 13. After tensile modulus tests, samples were taken.

The tensile modulus testing results from using the Testometric X350-20 equipment on PLA tensile test specimens are shown in the diagram below. Maintaining a infill density of 100%, the specimens were tested at various temperatures (20°C, 35°C, 40°C & 50°C) and infill orientations (0°, 90°).

Figure 14. Specimens after tensile modulus testing

The picture below displays the tensile modulus testing results obtained on PLA tensile test specimens using the Testometric X350-20 equipment. The specimens were examined with a infill density of 50% and at different temperatures (20°C, 35°C, 40°C & 50°C) and infill orientations (45°, -45°).

Figure 15. Specimens obtained after conducting tensile modulus testing

The image below illustrates the results of the tensile modulus testing conducted on PLA tensile test specimens using the Testometric X350-20 apparatus. The specimens were analysed using a infill density of 75% and were subjected to various temperatures (20°C, 35°C, 40°C & 50°C) and infill orientations (45°, -45°).

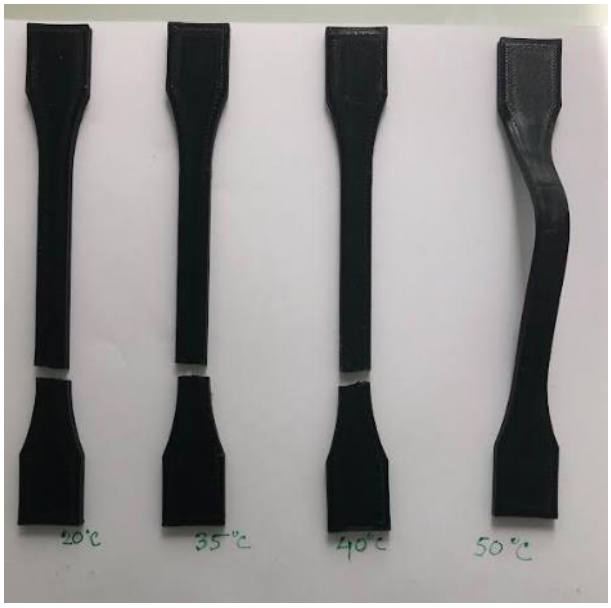

Figure 16. Specimens obtained after tests of the tensile modulus

The tensile modulus test results for PLA tensile test specimens utilising the Testometric X350-20 apparatus are shown in the image below. The samples were examined at infill density of 100% and exposed to infill orientations (45°, -45°) and different temperatures (20°C, 35°C, 40°C & 50°C)

Figure 17. Samples from tensile modulus tests

4.2 Tensile Modulus

The figure 18 indicates the stress (MPa) vs strain curve at 20°C and at different infill densities (50%, 75% and 100% respectively) of infill orientations (0°, 90°).

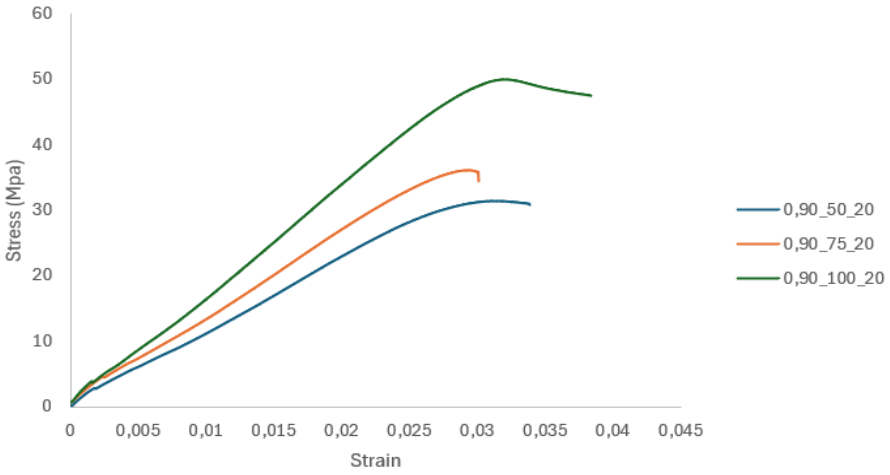

Figure 18. Typical stress vs strain curves of PLA at different densities and 20°C of I.0 (0°, 90°)

The graph labelled as 19 represents the relationship between stress (measured in MPa) and strain at a temperature of 35°C and three different infill densities (50%, 75%, and 100%) of infill orientations (0° and 90°).

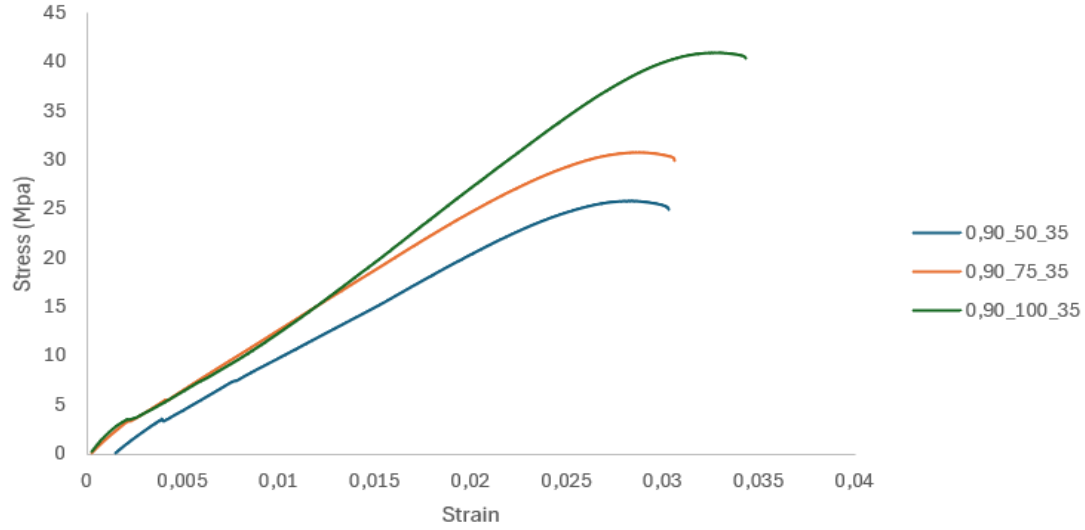

Figure 19. Typical stress vs strain curves of PLA at different densities and 35°C of I.0 (0°, 90°)

The relationship between stress (measured in MPa) and strain at 40°C and three distinct infill densities (50%, 75% and 100%) of infill orientations (0° and 90°) is shown in the graph with the label 20.

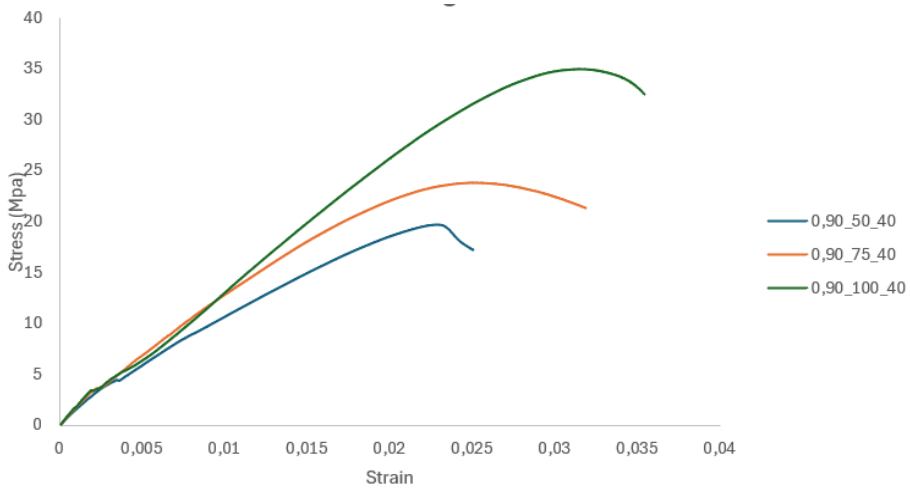

Figure 20. Typical stress vs strain curves of PLA at different densities and 40°C of I.0 (0°, 90°)

The graph with the label 21 illustrates the relationship between stress (measured in MPa) and strain at 50°C and three different infill densities (50%, 75% and 100%) of infill orientations (0° and 90°).

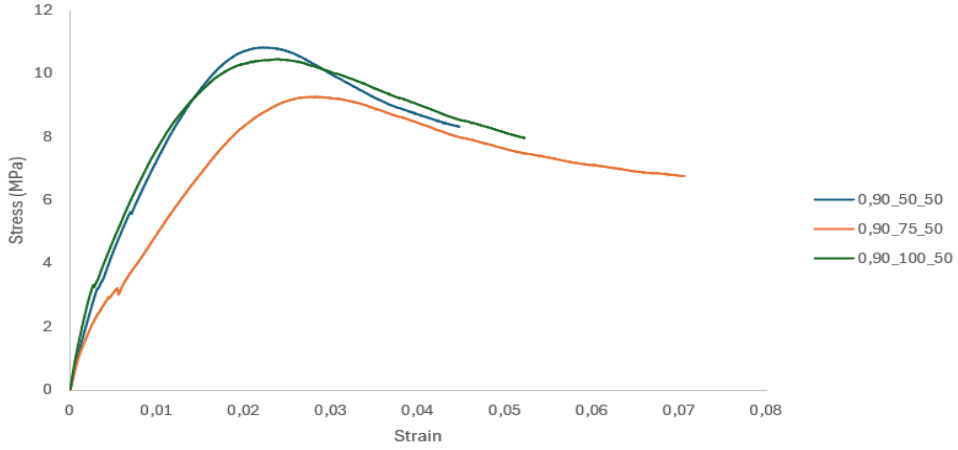

Figure 21. Typical stress vs strain curves of PLA at different densities and 50°C of I.0 (0°, 90°)

From the figure 18-21, the tensile modulus (TM) values of PLA at various temperatures (20°C, 35°C, 40°C, and 50°C) and infill densities (50%, 75%, and 100%) for infill orientation (0°, 90°) were calculated by the using of SFS-EN ISO-EN 527-1:2019 which was shown in Table 4.

From the straight-line portion of stress vs strain curve, σ_2 = 2,9450001 N, σ_1 =0,215 N, ε_2 =0,00285 mm and ε_1 = 0.000224 mm were found from infill orientation (0°, 90°) at 50% infill density and 50°C.

So, Tensile Modulus = (2,9450001-0,215) N/ (0,00285-0,000224) mm = 1039,5 MPa

Table 4. Tensile modulus (MPa) at different temperatures and densities (0°, 90° infill orientations)

% of infill Densities	TM (20°C)	TM (35°C)	TM (40°C)	TM (50°C)
50	1583,4	1348,3	1265,3	1039,5
75	1720,7	1647,1	1512,5	1387,4
100	2233,74	1999,7	1993,9	1811,4

The relationship between stress (measured in MPa) and strain at 20°C and three distinct infill densities (50%, 75%, and 100%) of infill orientations (45° and -45°) is shown in the graph with the label 22.

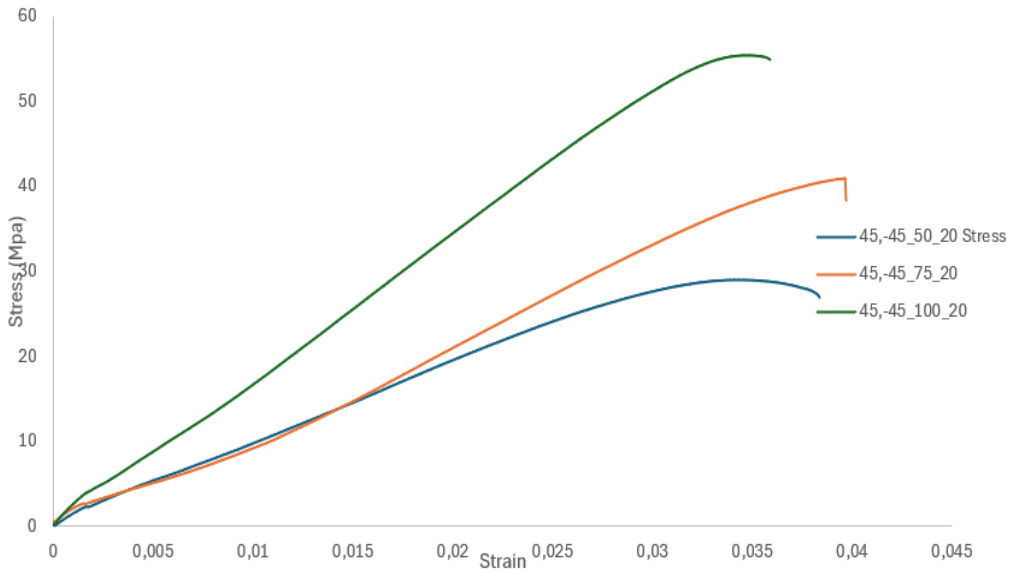

Figure 22. Typical stress vs strain curves of PLA at different densities and 20°C of I.0 (45°, -45°)

The graph labelled 23 illustrates the correlation between stress (measured in MPa) and strain at a temperature of 35°C. The data includes three different infill densities (50%, 75%, and 100%) and infill orientations (45° and -45°).

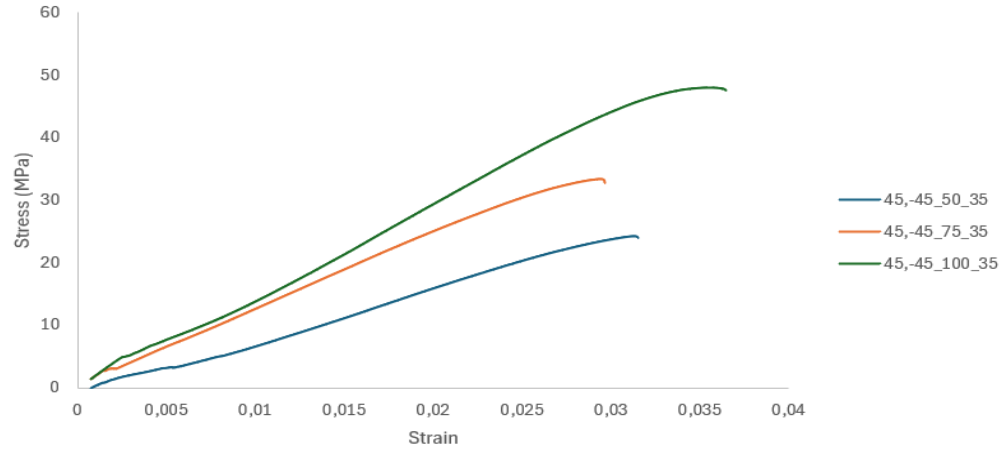

Figure 23. Typical stress vs strain curves of PLA at different densities and 35°C of I.0 (45°, -45°)

The correlation at 40°C between strain and stress (measured in MPa) is shown in the graph designated 24. Three distinct infill densities (50%) 75%, and 100% as well as infill orientations (45° and -45°) are included in the data.

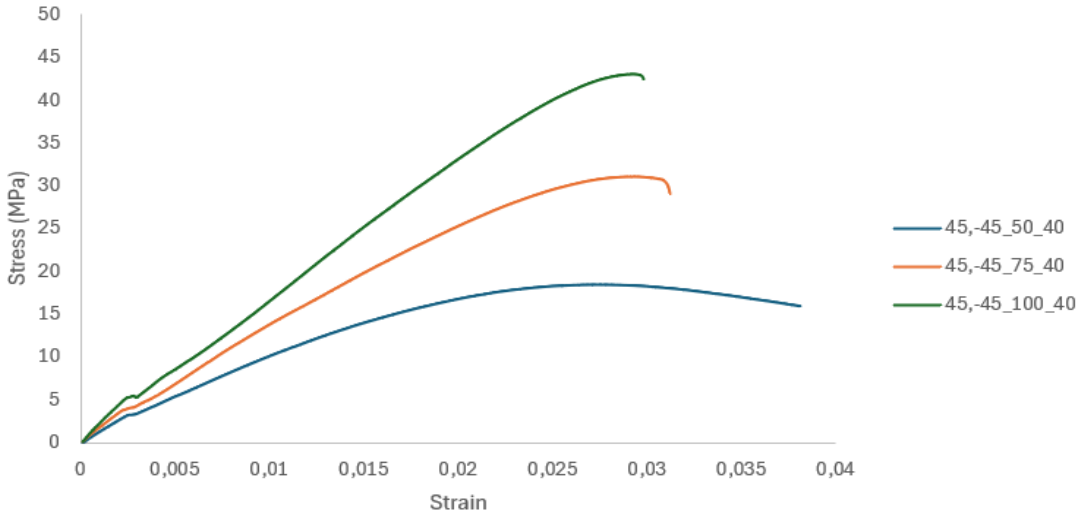

Figure 24. Typical stress vs strain curves of PLA at different densities and 40°C of I.0 (45°, -45°)

At 50°C, the graph 25 shows the relationship between strain and stress, which is recorded in MPa. The data includes three different infill densities: 50%, 75%, and 100%. It also includes infill orientations (45°, -45°).

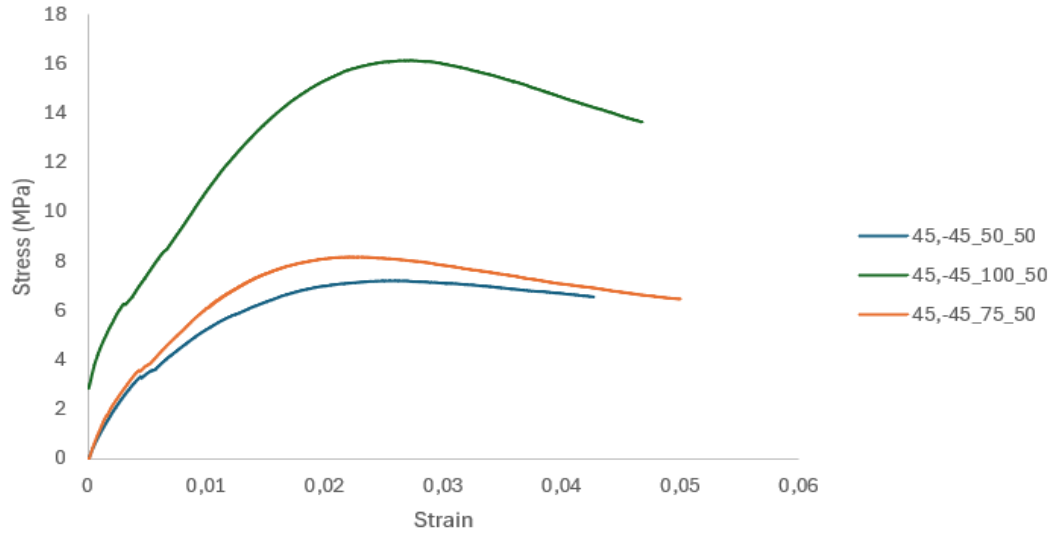

Figure 25. Typical stress vs strain curves of PLA at different densities and 50°C of I.0 (45°, -45°)

The SFS-EN ISO-EN 527-1:2019 was used to measure the tensile modulus. From the figure 22-25, the tensile modulus (TM) values of PLA at various temperatures (20°C, 35°C, 40°C, and 50°C) and infill densities (50%, 75%, and 100%) for infill orientation (45°, -45°) were calculated which was shown in Table 5.

Table 5. Tensile modulus (MPa) at different temperatures and infill densities (45°, -45° infill orientations)

% of Infill Densities	TM (20°C)	TM (35°C)	TM (40°C)	TM (50°C)
50	1497,6	1298,1	1249,3	1017,2
75	1694,2	1539,2	1497,8	1329,1
100	2084,3	1982,9	1872,9	1636,7

4.3 Yield Strength

The yield strengths were calculated from the stress vs strain curves. The Tables 6 and 7 detail the yield strength (YS) values of PLA at various temperatures and infill densities for two different orientations: (0°, 90°) and (45°, -45°).

Figure 26 indicates how Yield strength (MPa) was found from stress vs strain curve using the offset formula procedure. SFS-EN ISO-EN 527-1:2019 method was used to calculate the yield strength. The stress value of the intersection point is known as Yield strength (MPa) which is 6,05 MPa. The data were taken from infill orientation (0°, 90°) at infill density 50% and temperature 50°C respectively.

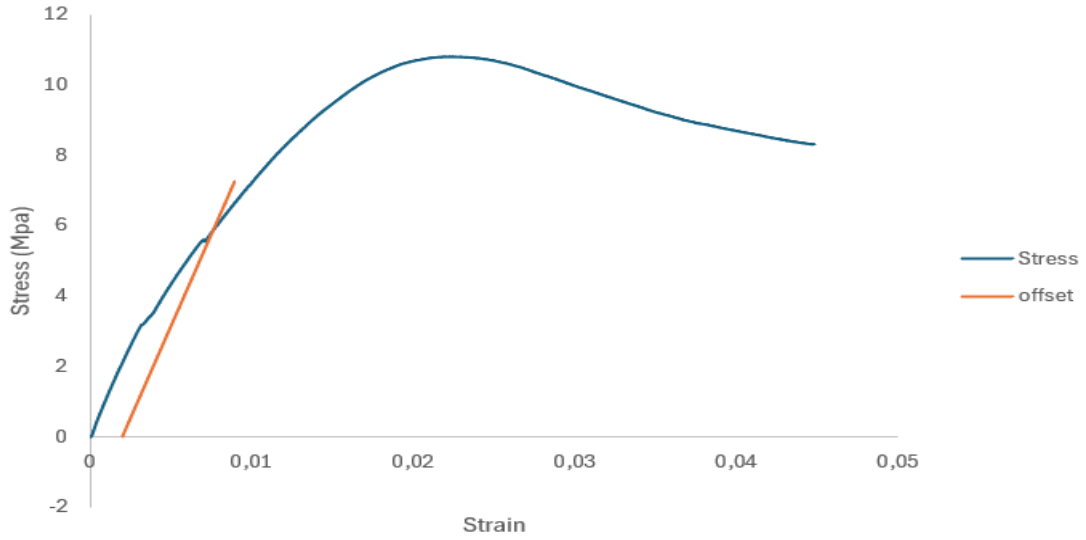

Figure 26. Stress vs strain curve at infill density 50% and 50°C of infill orientation (0°, 90°)

Table 6. Yield strength (YS) at different temperatures and infill densities (0°, 90° infill orientations)

% of Infill Densities	YS (20°C)	YS (35°C)	YS (40°C)	YS (50°C)
50	8,26	7,89	6,81	6,05
75	12,5	11,1	10,62	9,65
100	12.93	12,78	10,85	10,12

Table 7. Yield strength (YS) at different temperatures and infill densities (45°, -45° infill orientations)

% of Infill Densities	YS (20°C)	YS (35°C)	YS (40°C)	YS (50°C)
50	6,89	5,91	5,73	5,64
75	10.37	10,35	9,70	8,15
100	11,16	9,8	9,19	8,9

4.4 Tensile Modulus vs Temperature

The figure 27 indicates the Tensile Modulus (MPa) vs Temperature (°C) curve at different infill densities (50%, 75% and 100% respectively) of infill orientations (0°, 90°).

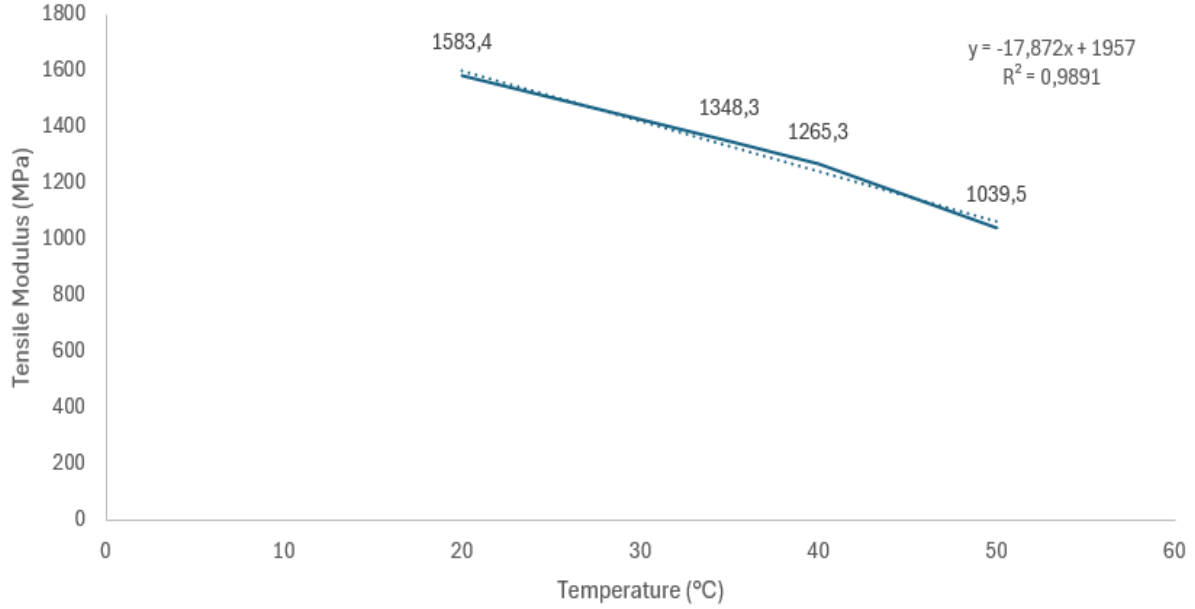

(a)

‘

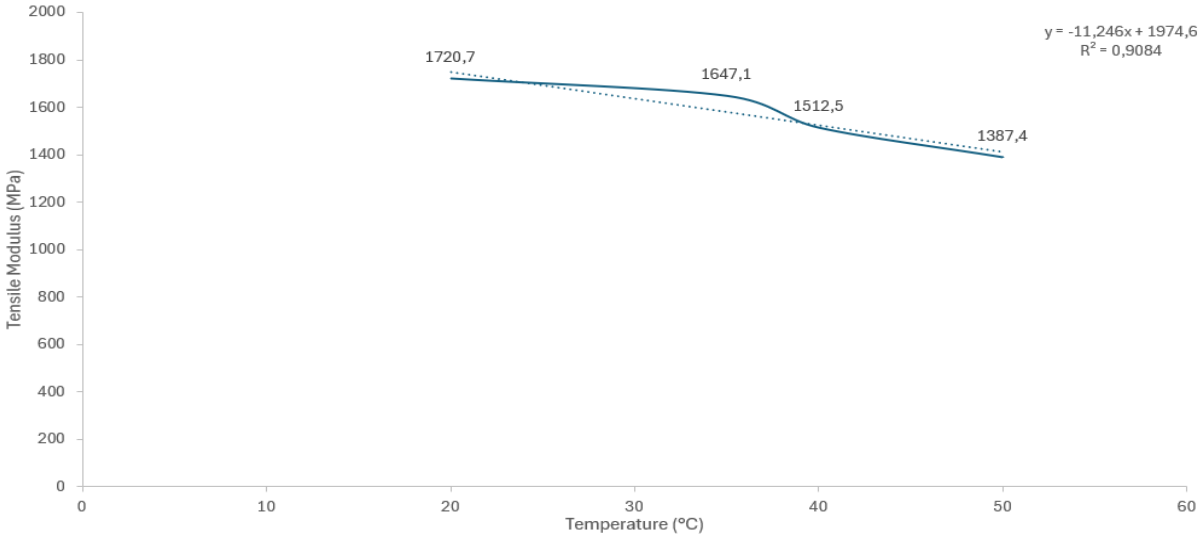

(b)

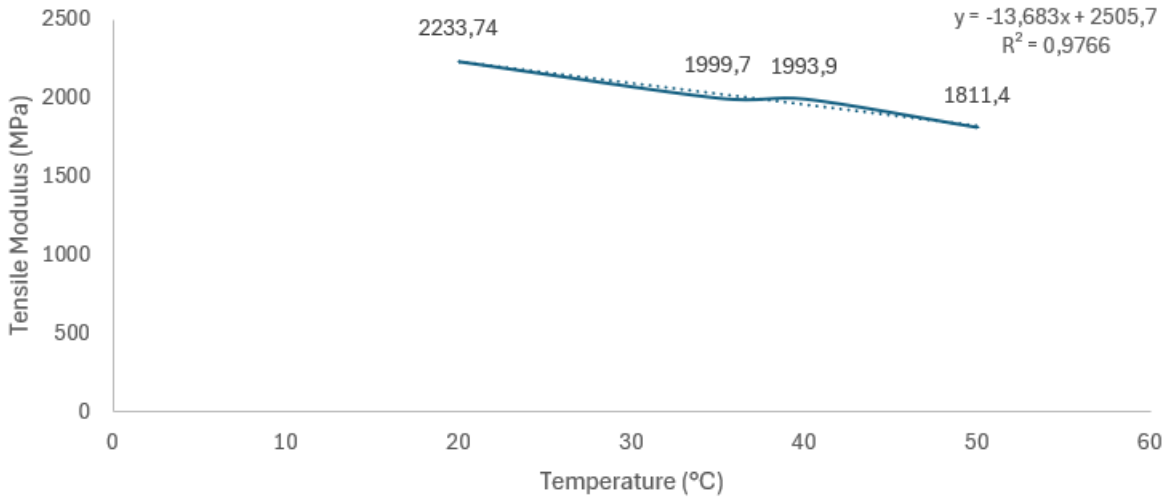

(c)

Figure 27. Tensile Modulus (MPa) vs Temperature (°C) curves of PLA at (a) 50% infill density, (b) 75% infill density and (c) 100% infill density of infill orientations (0°, 90°)

The figure 28 illustrates the Tensile Modulus (MPa) vs Temperature (°C) curve at different infill densities (50%, 75% and 100% respectively) of infill orientations (45°, -45°).

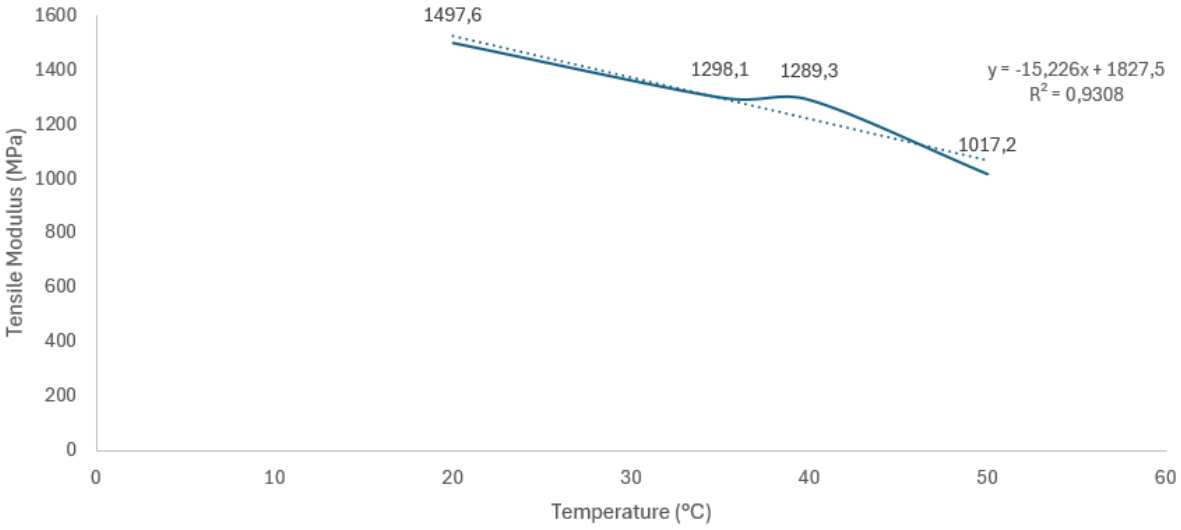

(a)

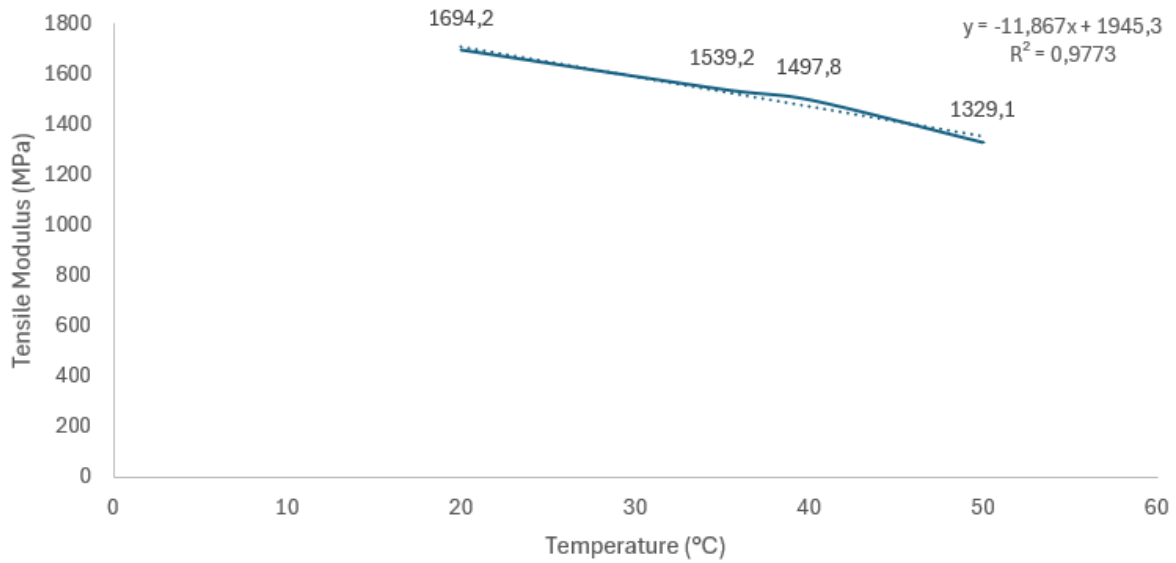

(b)

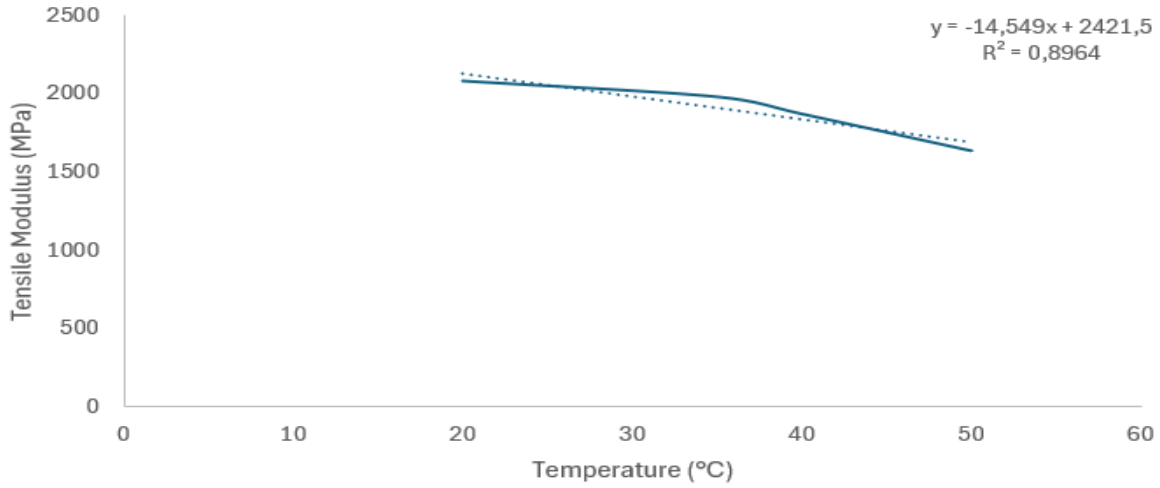

(c)

Figure 28. Tensile Modulus (MPa) vs Temperature (°C) curves of PLA at (a) 50% infill density, (b) 75% infill density and (c) 100% infill density of infill orientations (45°, -45°)

Table 8 indicates all the mechanical constants at different infill orientations, infill densities and temperatures. The negative slop coefficient (for example: - 17,872) is expressed by A, which indicates the strong relationship between tensile modulus and temperature and C indicates the estimated value of tensile modulus at 0°C.

Table 8. Mechanical constants (Tensile Modulus) at different I.O, I.D and Temperatures.

Mechanical Constants	50% I. D	75% I. D	100% I. D
A (MPa/°C) at I.O (0°,90°)	-17,872	-11,246	-13,683
C (MPa) at I.O (0°, 90°)	1957	1974,6	2505,7
A (MPa/°C) at I. O (45°, -45°)	-15,226	-11,867	-14,549
C (MPa) at I.O (45°, -45°)	1827,5	1945,3	2421,5

4.5 Yield Strength vs Temperature

The figure 29 illustrates the Yield Strength (MPa) vs Temperature (°C) curve at different infill densities (50%, 75% and 100% respectively) of infill orientations (0°, 90°).

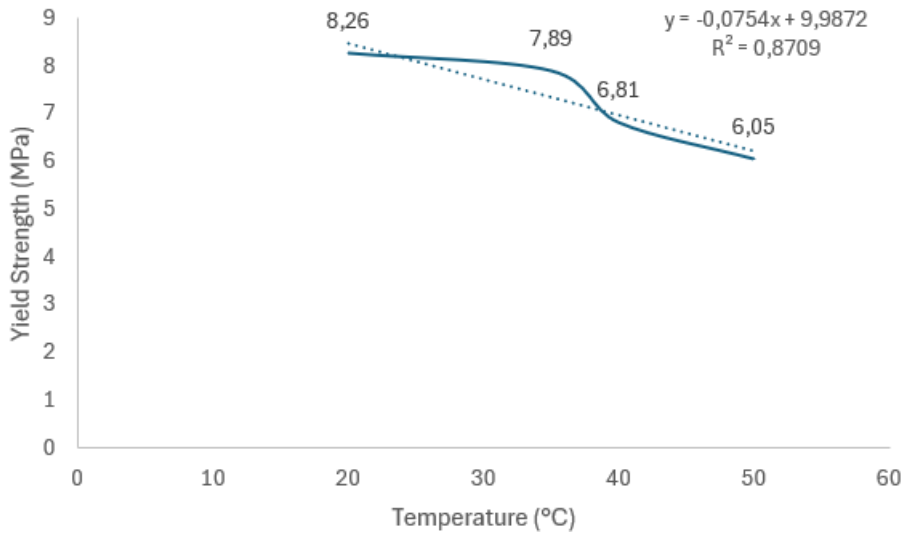

(a)

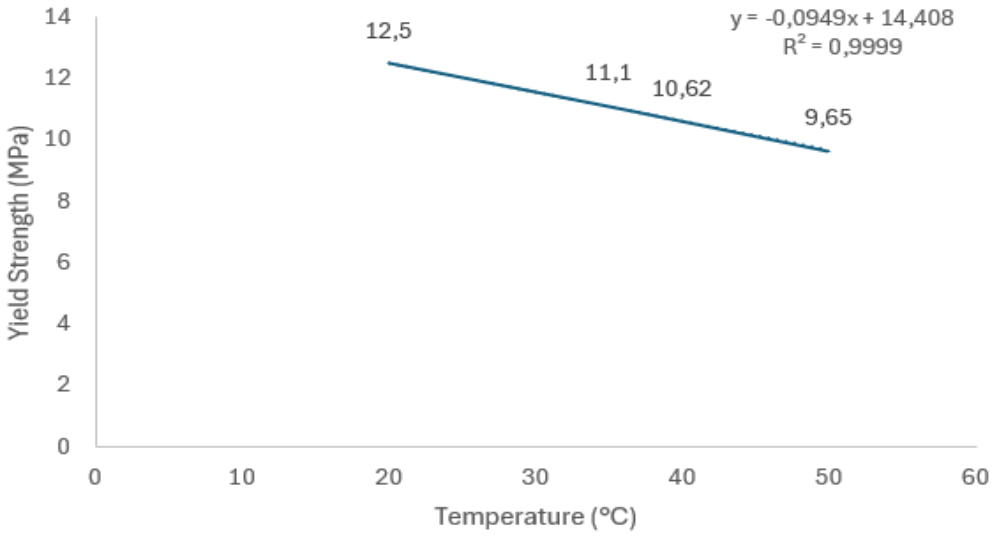

(b)

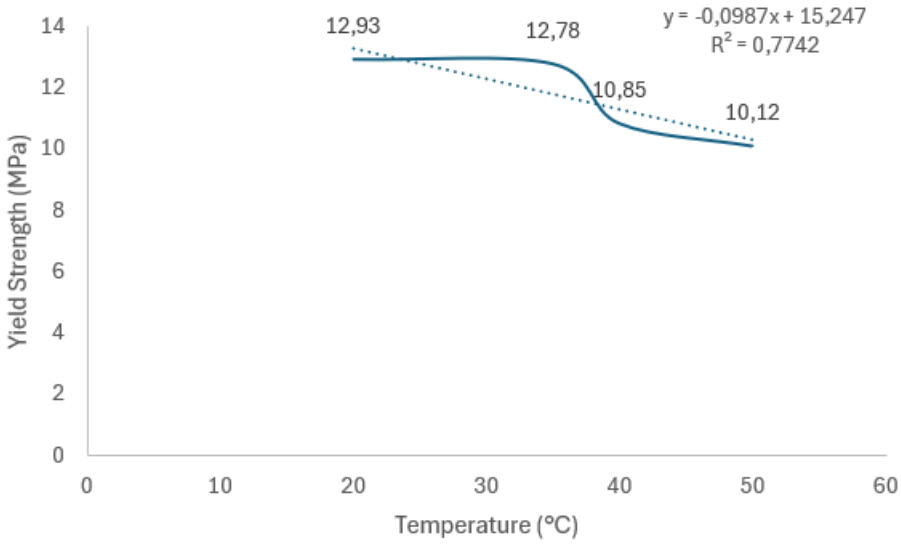

(c)

Figure 29. Yield Strength (MPa) vs Temperature (°C) curves of PLA at (a) 50% infill density, (b) 75% infill density and (c) 100% infill density of infill orientations (0°, 90°)

The figure 30 indicates the Yield Strength (MPa) vs Temperature (°C) curve at different infill densities (50%, 75% and 100% respectively) of infill orientations (45°, -45°).

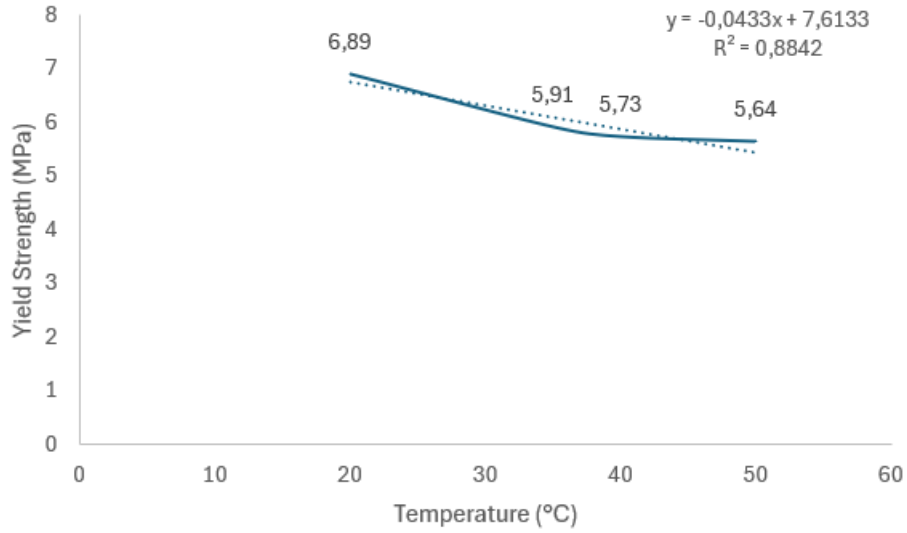

(a)

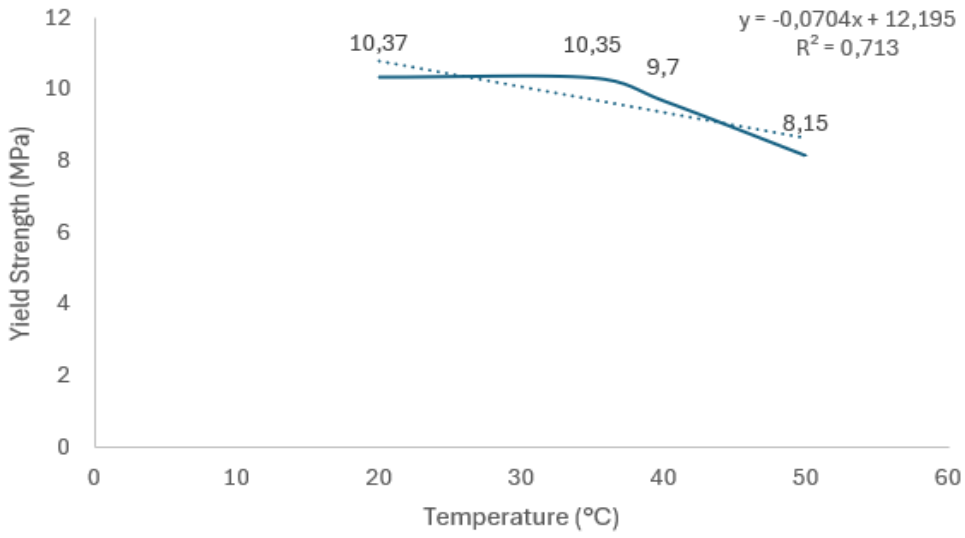

(b)

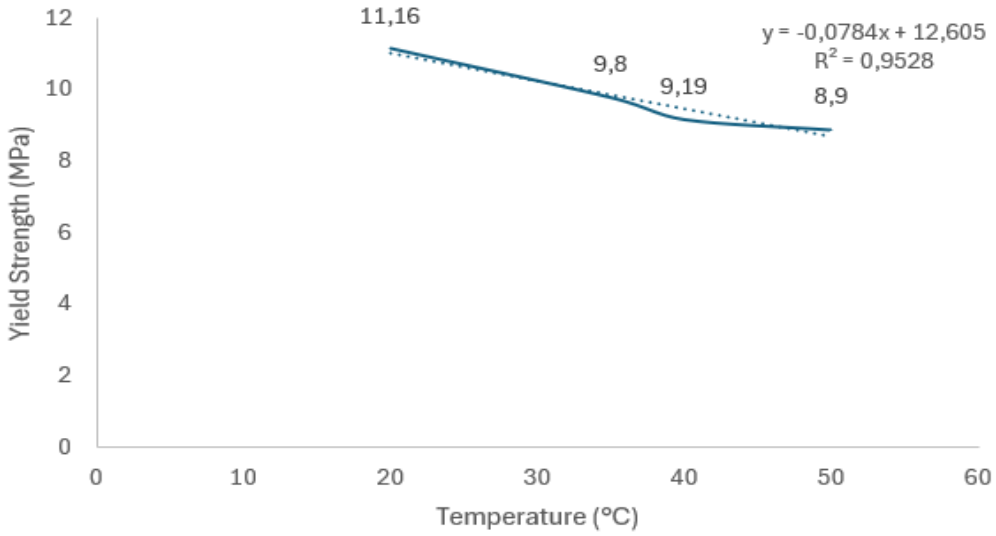

(c)

Figure 30. Yield Strength (MPa) vs Temperature (°C) curves of PLA at (a) 50% infill density, (b) 75% infill density and (c) 100% infill density of infill orientations (45°, -45°)

Table 9 indicates all the mechanical constants at different infill orientations, infill densities and temperatures. The negative slop coefficient (such as: - 0,0754) is expressed by B, which indicates the strong relationship between yield strength and temperature and D indicates the estimated value of yield strength at 0°C.

Table 9. Mechanical constants (Yield Strength) at different I.O, I.D and Temperatures.

Mechanical Constants	50% I. D	75% I. D	100% I. D
B (MPa/°C) at I.O (0°,90°)	-0,0754	-0.0949	-0,0949
D (MPa) at I.O (0°, 90°)	9,9872	14,408	15,247
B (MPa/°C) at I. O (45°, -45°)	-0,0433	-0,0704	-0,0784
D (MPa) at I.O (45°, -45°)	7,6133	12,195	12,605

5 DISCUSSIONS

The figure 31 shows the comparison of Tensile modulus (MPa) of two different infill orientations (0°, 90°) and (45°, -45°) at four different Temperatures (20°C, 35°C, 40°C and 50°C) and three different infill densities (50%, 75% and 100%).

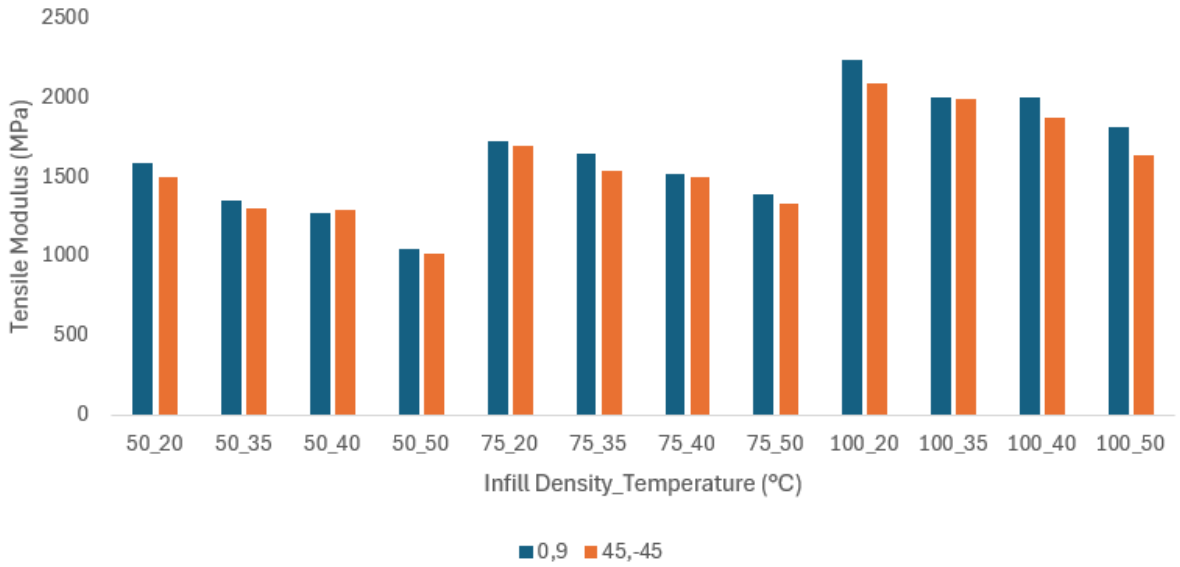

Figure 31. Comparison Tensile modulus of infill orientations (0°, 90°) and (45°, -45°) at different temperatures and different infill densities.

It is clearly showed that from the above figure, at 20°C, the tensile modulus increases with increase infill density for both infill orientations (0°, 90°) and (45°, -45°). Higher densities result in higher stiffness due to a greater proportion of crystalline structures in PLA.

Like the trend at 20°C, increasing the infill density at 35°C also leads to higher tensile modulus values for both infill orientations. The data indicates that higher infill densities contribute to improved mechanical properties, maintaining structural integrity under moderate temperature conditions.

At 40°C, the tensile modulus continues to increase with infill density, although there is a notable decrease in stiffness compared to lower temperatures. For 50% density, the tensile modulus is lower at the (0°, 90°) infill orientation compared to the (45°, -45°) infill orientation,

suggesting that certain orientations may distribute loads more effectively at elevated temperatures.

At 50°C, the tensile modulus further increases for both infill orientations and all infill densities. The (0°, 90°) infill orientation consistently shows higher tensile modulus values compared to the (45°, -45°) orientation, indicating better load-bearing capacity.

This is consistent with previous research and theory, which serves as a foundation for creating PLA materials with precise mechanical properties. The study emphasizes that the (0°, 90°) infill orientation greatly enhances stiffness and load-bearing capacity by aligning more effectively with the direction of tensile force, hence decreasing deformation. In contrast, the infill orientation at (45°, -45°) experiences higher levels of shear deformation and less effective load transfer, leading to a reduced tensile modulus.

The figure 32 shows the comparison of Yield strength (MPa) of two different infill orientations (0°, 90°) and (45°, -45°) at four different Temperatures (20°C, 35°C, 40°C and 50°C) and three different infill densities (50%, 75% and 100%).

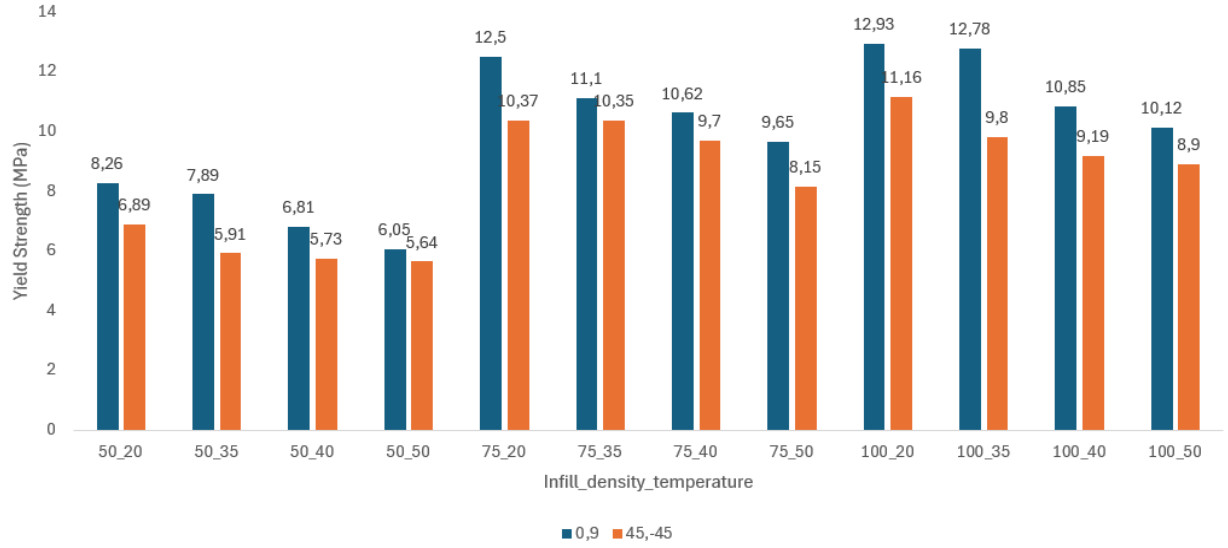

Figure 32. Comparison Yield strength of infill orientations (0°, 90°) and (45°, -45°) at different temperatures and different infill densities.

Figures 32 depict the yield strength as a function of temperature for various infill densities and infill orientations. The yield strength decreases with increases temperatures. The (0°, 90°) infill orientation consistently shows higher yield strength compared to (45°, -45) infill orientation. It is also shown that the yield strengths decrease as the temperature increases for both infill orientations. Indicates that High temperatures diminish PLA's molecular mobility, reducing yield strengths. As temperature rises, PLA's amorphous areas become more flexible, making stress deformation easier. Temperatures can also disturb PLA's crystalline areas, reducing its structure. Low yield strengths originate from thermal softening, which diminishes material resistance to applied forces. As temperature rises, PLA loses mechanical integrity, making it unsuitable for high-temperature applications.

Tensile modulus against temperature graph for 50%, 75% and 100% PLA infill density at (0°, 90°) and (45°, -45°) infill orientations are described a relationship with the equations in the figures (27 & 28). Analysing the regression of the Tensile modulus versus temperature curve for various infill densities and orientations aids in comprehending and forecasting the impact of these variables on material performance. This research assists in optimising material qualities for applications, guaranteeing dependability, and improving the efficiency of 3D-printed structures when subjected to heat stress. From the regression it is clearly observed that infill orientation (0°, 90°) provides better load distribution at elevated temperatures. This implies that the best infill arrangements for improved material stability and performance in hot conditions.

The figure 33 indicates the Tensile Modulus (MPa) vs Temperature (°C) curve at infill density 50% of infill orientations (0°, 90°). The tensile modulus values were considered for the temperature 20°C to 50°C with 1°C interval in this figure.

From the figure 27 (a), a regression equation (-17,9724x+1957, R^2 =0,9897) is found. From this equation the tensile modulus will be calculated for the temperature range 20°C- 50°C.
For example-
For 20°C: -17,9724*20 +1957 = 1597, 552 MPa.
For 21°C: -17,9724*21 +1957 = 1579,5796 MPa.
For 50°C: -17,9724*50 +1957 = 1058,38 MPa.

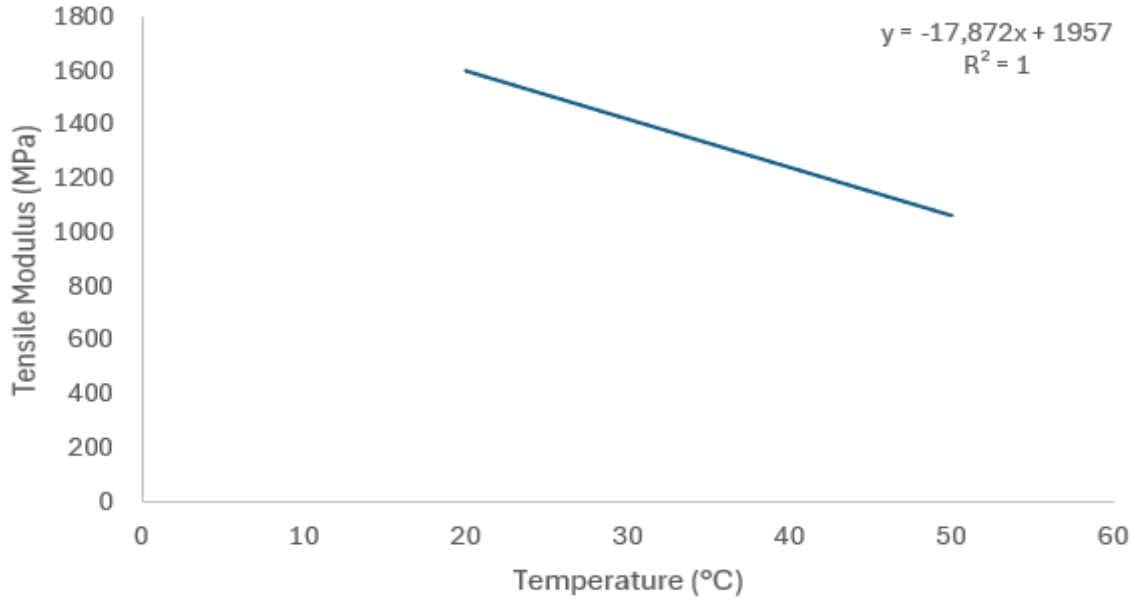

Figure 33. Tensile Modulus (MPa) vs Temperature (°C) curves of PLA at 50% infill density of infill orientations (0°, 90°).

The linear equation y = -17,872x + 1957, R^2 = 1 represents the relationship between temperature and tensile modulus which provides important information about the mechanical properties of PLA. The high R^2 value indicates that temperature has a substantial impact on tensile modulus, enabling precise predictions of material behaviour by considering temperature fluctuations.

Over the investigated range from 20°C to 50°C, there is a strong inverse relationship between tensile modulus and temperature, as indicated by the negative slope coefficient (-17,872). It implies that the tensile modulus decreases linearly with temperature. It provides an accurate quantitative explanation of how PLA's tensile modulus changes with temperature.

Yield strength vs temperature graph for 50%, 75% and 100% PLA infill density at (0°, 90°) and (45°, -45°) infill orientations are shown a relationship with the equations in the figures (29-30). The objective is to measure the correlation between temperature and yield strength by regression analysis of the Yield strength vs. temperature curve for various infill densities and infill orientations. This facilitates the prediction of material behaviour, optimisation of design parameters, and guarantee of structural integrity and performance in 3D-printed components under different heat conditions.

The figure 34 illustrates the Yield Strength (MPa) vs Temperature (°C) curve at infill density 50% of infill orientations (0°, 90°). The yield strength values were considered for the temperature 20°C to 50°C with 1°C interval in this figure.

From the figure 29 (a), a regression equation (-0,0754x+9,9872, R^2 =0,8709) is found. From this equation the yield strength will be calculated for the temperature range 20°C- 50°C.
For example-
For 20°C: -0,0754*20 +9,9872 = 8,4792 MPa.
For 21°C: -0,0754*21 +9,9872 = 8,4038 MPa.
For 50°C: -0,0754*50 +9,9872 = 6,2172 MPa.

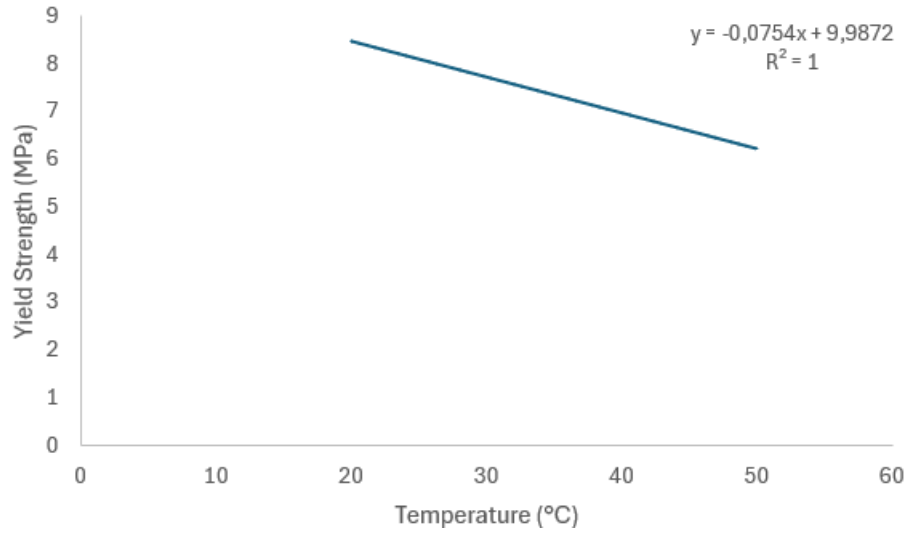

Figure 34. Yield Strength (MPa) vs Temperature (°C) curves of PLA at 50% infill density of infill orientations (0°, 90°)

From the above figure the equation y = −0,0754x+9,9872, R^2 =1 is observed which provides critical insights into the mechanical behaviour of PLA.The regression study of yield strength vs. temperature shows that for every degree rise in temperature, yield strength drops by 0,0754 units. The strong alignment between the data and the linear model (R^2 =1) highlights the precision and dependability of the observed correlation. This relation shows how important it is to think about thermal effects when designing and using materials with different infill densities and orientations.

From this thesis, it is clearly shown that the tensile modulus decreases as increases the temperatures. The same results are observed in the other research articles. All the tensile modulus increases with increases the percentages of infill densities which shows same results of other scientific articles. Except one case, all tensile modulus shows higher values for the infill orientation (0°, 90°) compared to the infill orientation (45°, -45) which also indicates same scenario of other research articles.

This thesis clearly demonstrates that the yield strengths drop as the temperatures increase. This is inherent. Similar findings are evident in the other scholarly publications. The yield strength increases as the percentages of infill densities grow, which aligns with the findings of other research studies. Moreover, the yield strength is higher for the infill orientations of (0°, 90°) compared to the infill orientations of (45°, -45°), as seen in other study publications.

6 CONCLUSIONS

This thesis examines the effect of temperature on the mechanical properties of 3D printed Polylactic Acid (PLA). The tensile specimens were designed according to the ISO 527 2/1B standard and printed using a Creality Ender-3 Pro 3D printer employing Fused Deposition Modelling (FDM) technology. The infill orientations of the specimens were set at (0°, 90°) and (45°, -45°), and three different infill densities of 50%, 75%, and 100% were used.

The investigation provided substantial insights into the relationship between temperature and the tensile modulus and yield strength of PLA. The tensile modulus exhibited a linear decline with increasing temperature for both (0°, 90°) and (45°, -45°) infill orientations across the different densities.

Similarly, the yield strength also showed a decline with increasing temperature for both (0°, 90°) and (45°, -45°) infill orientations across the different infill densities.

The comparative analysis revealed that the (0°, 90°) infill orientation provided higher tensile modulus and yield strength compared to infill orientation (45°, -45°). The tensile modulus and yield strength rises as rises the percentages of infill densities. Apart from one case, the infill orientation (0°, 90°) provides higher tensile modulus compared to the infill orientation (45°, -45°).

Overall, the higher tensile modulus (2233,74 MPa) is observed at 100% infill density and 20°C for infill orientation (0°, 90°). The greater tensile modulus (2084,3 MPa) is noted at infill orientations of (45°, -45°) and 100% infill density at 20°C. The maximum yield strength of 12,93 MPa is achieved when the infill density is 100% and the infill orientation (0°,90°) at a temperature of 20°C. The highest yield strength, measured at 11,16 MPa, is observed when the infill orientations are set at (45°, -45°) and the infill density is set to 100%, all at a temperature of 20°C.

Moreover, the findings of this study highlight the significant impact of temperature on the mechanical properties of 3D printed PLA. These insights are crucial for optimizing material

performance in practical applications and ensuring their reliability under varying temperature conditions.

While significant progress has been made in understanding the impact of printing temperature and infill density on tensile modulus and yield strength, there are still areas that require further investigation. Future research should focus on developing adaptive and real-time optimization techniques for temperature and infill density during the printing process can improve the quality and consistency of 3D printed parts. Machine learning and AI-driven approaches hold promise for dynamically adjusting printing parameters to achieve optimal mechanical properties

References

Abeykoon, C., Sri-Amphorn, P., & Fernando, A. (2020). Optimization of fused deposition modeling parameters for improved PLA and ABS 3D printed structures. *International Journal of Lightweight Materials and Manufacture*, *3*(3), 284–297. https://doi.org/10.1016/j.ijlmm.2020.03.003

Ahmad, M. N., & Yahya, A. (2023). Effects of 3D Printing Parameters on Mechanical Properties of ABS Samples. https://doi.org/10.20944/preprints202310.0656.v1

Algarni, M., & Ghazali, S. (2021). Comparative Study of the Sensitivity of PLA, ABS, PEEK, and PETG's Mechanical Properties to FDM Printing Process Parameters. *Crystals*, *11*(8), 995. https://doi.org/10.3390/cryst11080995

Alhazmi, M. W., & Backar, A. (2020). Influence of Infill density and Orientation on the Mechanical Response of PLA+ Specimens Produced using FDM 3D Printing. *International Journal of Advanced Science and Technology*, 29 (6), 3362-3371.

Ali, M. H., Katsuki, A., Kurokawa, S., & Sajima, T. (2013). Design of Mechanical Actuator in 3D CAD Software. *Procedia Engineering*, *64*, 473–478. https://doi.org/10.1016/j.proeng.2013.09.121

Ambati, S. S., & Ambatipudi, R. (2022). Effect of infill density and infill pattern on the mechanical properties of 3D printed PLA parts. *Materials Toddy: Proceedings*, *64*, 804–807. https://doi.org/10.1016/j.matpr.2022.05.312

Antanitta S, V., Patadiya, J., & Kandasubramanian, B. (2024). Biopolymer-chitin products by direct ink writing (DIW): A review. *Hybrid Advances*, 5(100115). https://doi.org/10.1016/j.hybadv.2023.100115

Bakar, A. a. B. A., Zainuddin, M. Z. B., Adam, A. N. B., Noor, I. S. B. M., Tamchek, N. B., Alauddin, M. S. B., & Ghazali, M. I. B. M. (2022). The study of mechanical properties of poly(lactic) acid PLA-based 3D printed filament under temperature and environmental conditions. *Materials Today: Proceedings*, *67*, 652–658.https://doi.org/10.1016/j.matpr.2022.06.198

Baniasadi, H., Abidnejad, R., Fazeli, M., Lipponen, J., Niskanen, J., Kontturi, E., Seppälä, J., & Rojas, O. J. (2024). Innovations in hydrogel-based manufacturing: A comprehensive review of direct ink writing technique for biomedical applications. *Advances in Colloid and Interface Science*, *324*, 103095. https://doi.org/10.1016/j.cis.2024.103095

Calles, A. F., Carou, D., & Ferreira, R. T. L. (2021). Experimental Investigation on the Effect of Carbon Fiber Reinforcements in the Mechanical Resistance of 3D Printed Specimens. *Applied Composite Materials* 29:937-952. https://doi.org/10.1007/s10443-021-09996-7

Cantrell, J., Rohde, S., Damiani, D., Gurnani, R., DiSandro, L., Anton, J., Young, A., Jerez, A., Steinbach, D., Kroese, C., & Ifju, P. (2016). Experimental Characterization of the Mechanical Properties of 3D Printed ABS and Polycarbonate Parts. In *Conference proceedings of the Society for Experimental Mechanics* (pp. 89–105). https://doi.org/10.1007/978-3-319-41600-7_11

Chacón, J. M., Caminero, M. A., García-Plaza, E., & Núñez, P. J. (2017). Additive manufacturing of PLA structures using fused deposition modelling: Effect of process parameters on mechanical properties and their optimal selection. *Materials & Design*, 124, 143-157. https://doi.org/10.1016/j.matdes.2017.03.065

Chhabra, D. (2017). Comparison ana analysis of different 3d printing techniques. https://doi.org/10.21172/1.841.44

Das, A., Awasthi, P., Jain, V., & Banerjee, S. S. (2023). 3D printing of maxillofacial prosthesis materials: Challenges and opportunities. *Bioprinting*, *32*, e00282. https://doi.org/10.1016/j.bprint.2023.e00282

Ender-3 Pro 3D Printer. (n.d.). Creality. https://www.creality.com/products/ender-3-pro-3d-printer

E5AC | Omron. (n.d.). https://automation.omron.com/en/us/products/family/E5AC/e5ac-rr4a5m-009

Ferreira, R. T. L., Amatte, I. C., Dutra, T. A., & Bürger, D. (2017). Experimental characterization and micrography of 3D printed PLA and PLA reinforced with short carbon fibers. *Composites. Part B, Engineering*, *124*, 88–100. https://doi.org/10.1016/j.compositesb.2017.05.013

Foltuţ, D., Vălean, E., Dzitac, V., & Marşavina, L. (2023). The influence of temperature on the mechanical properties of 3D printed and injection molded ABS. *Materials Today: Proceedings*, 78, 210–213. https://doi.org/10.1016/j.matpr.2022.10.039

Ganeshkjumar, S., Kumar, S. D., Magarajan, U., Sivanraju, R., Arulmurugan, B., Sharma, S., Li, C. H., A, I. R., & Badran, M. (2022). Investigation of Tensile Properties of Different infill Pattern Structures of 3D-Printed PLA Polymers: Analysis and Validation Using Finite Element Analysis in ANSYS. *Materials* 15(15):5142. https://doi.org/10.3390/ma15155142

Gebrehiwot, S. Z., Leal, L. E., Eickhoff, J. N., & Rechenberg, L. (2020). The influence of stiffener geometry on flexural properties of 3D printed polylactic acid (PLA) beams. *Progress in Additive Manufacturing*, *6*(1), 71–81. https://doi.org/10.1007/s40964-020-00146-2

Gebrehiwot, S. Z., Espinosa-Leal, L., Linderbäck, P., & Remes, H. (2023). Optimising the mechanical properties of additive-manufactured recycled polylactic acid (rPLA) using single and multi-response analyses methods. *The International Journal of Advanced Manufacturing Technology/International Journal, Advanced Manufacturing Technology*, 129(11–12), 4909–4924. https://doi.org/10.1007/s00170-023-12623-3

Gebrehiwot, S. Z., Espinosa-Leal, L., Andersson, M., & Remes, H. (2023). On the Short-Term Creep and Recovery Behaviors of Injection Molded and Additive-Manufactured Tough Polylactic Acid Polymer. *Journal of Materials Engineering and Performance*, *32*(22), 10412–10430. https://doi.org/10.1007/s11665-023-08278-6

Geyer, R., Jambeck, J. R., & Law, K. L. (2017). Production, use, and fate of all plastics ever made. *Science Advances*, *3*(7). https://doi.org/10.1126/sciadv.1700782

Goh, G. D., & Yeong, W. Y. (2022). Applications of machine learning in 3D printing. *materialstoday: Proceedings*, 70, 95-100. https://doi.org/10.1016/j.matpr.2022.08.551

Grant, I. S., & Phillips, W. R. (2001). *The elements of physics*. Oxford University Press

Guduru, K., & Srinivasu, G. (2020). Effect of post treatment on tensile properties of carbon reinforced PLA composite by 3D printing. *Materials Today: Proceedings*, *33*, 5403–5407. https://doi.org/10.1016/j.matpr.2020.03.128

Hadi, A., Kadauw, A., & Zeidler, H. (2023). The effect of printing temperature and moisture on tensile properties of 3D printed glass fiber reinforced nylon 6. *Materials Today: Proceedings*, 91, 48-55. www.elsevier.com/locate/matpr

Hasan, M. R., Davies, I. J., Pramanik, A., John, M., & Biswas, W. K. (2024). Potential of Recycled PLA in 3D Printing: A Review. *Sustainable Manufacturing and Service Economics*, *3*, 100020. https://doi.org/10.1016/j.smse.2024.100020

Hull, C. (1983). U.S. Patent No. 4,575,330. U.S. Patent and Trademark Office. Retrieved from https://patents.google.com/patent/US4575330A/en

Idumah, C. I., & Nwuzor, I. C. (2019). Novel trends in plastic waste management. *SN Applied Sciences/SN Applied Sciences*, *1*(11). https://doi.org/10.1007/s42452-019-1468-2

Jayanth, N., Jaswanthraj, K., Sandeep, S., Mallaya, N. H., & Siddharth, S. R. (2021). Effect of heat treatment on mechanical properties of 3D printed PLA. *Journal of the Mechanical Behavior of Biomedical Materials/Journal of Mechanical Behavior of Biomedical Materials*, *123*, 104764. https://doi.org/10.1016/j.jmbbm.2021.104764

Joseph, T. M., Kallingal, A., Suresh, A. M., Mahapatra, D. K., Hasanin, M., Haponiuk, J. T., & Thomas, S. 3D printing of polylactic acid: recent advances and opportunities. *The International Journal of Advanced Manufacturing Technology*, 125(21):1-21. https://doi.org/10.1007/s00170-022-10795-y

Kharat, V. J., Singh, P., Raju, G. S., Yadav, D. K., SatyanarayanaGupta, M., Arun, V., Majeed, A. H., & Singh, N. (2023c). Additive manufacturing (3D printing): A review of materials, methods, applications and challenges. *Materials Today: Proceedings.* https://doi.org/10.1016/j.matpr.2023.11.033

Maqsood, N., & Rimašauskas, M. (2021). Characterization of carbon fiber reinforced PLA composites manufactured by fused deposition modeling. *Composites. Part C, Open Access*, *4*, 100112. https://doi.org/10.1016/j.jcomc.2021.100112

Melentiev, R., Melentieva, M., & Yu, N. (2024). Top 10 Directions in Lithography 3D Printing. Bioprinting, e00343. https://doi.org/10.1016/j.bprint.2024.e00343

Mustafa, S. N. I. S., Man, S. H. C., Hassan, A., Baharulrazi, N., & Mohamad, Z. (2021). Mechanical and Thermal Properties of Polylactic Acid/Liquid Epoxidized Natural Rubber/Graphene Oxide Composites. *DOAJ (DOAJ: Directory of Open Access Journals)*. https://doi.org/10.3303/cet2189074

Naik, M., Thakur, D., & Chandel, S. (2022). An insight into the effect of printing orientation on tensile strength of multi-infill pattern 3D printed specimen: Experimental study. *Materials Today: Proceedings*, *62*, 7391–7395. https://doi.org/10.1016/j.matpr.2022.02.305

Rajpurohit, S. R., & Dave, H. K. (2018). Analysis of tensile strength of a fused filament fabricated PLA part using an open-source 3D printer. *The International Journal of Advanced Manufacturing Technology/International Journal, Advanced Manufacturing Technology*, *101*(5–8), 1525–1536. https://doi.org/10.1007/s00170-018-3047-x

Rana, M. (2022). The influence of infill direction on the low cycle fatigue performance of 3D printed PLA polymer., Theseus. Available at: https://www.theseus.fi/handle/10024/788533 (Accessed: January 30, 2023)

Saini, G., Segaran, N., Mayer, J., Saini, A., Albadawi, H., & Oklu, R. (2021). Applications of 3D Bioprinting in Tissue Engineering and Regenerative Medicine. *Journal of Clinical Medicine*, 10(21):4966. https://doi.org/10.3390/jcm10214966

Shahrubudin, N., Lee, T., & Ramlan, R. (2019). An Overview on 3D Printing Technology: Technological, Materials, and Applications. Procedia Manufacturing, 35, 1286–1296. https://doi.org/10.1016/j.promfg.2019.06.089

The X350 Series of Universal Testing Machines. (n.d.). AZoM. https://www.azom.com/equipment-details.aspx?EquipID=7884

Tran, N. (2019) The impact of printing orientation on the tensile properties of parts printed by fused deposition modelling., Theseus. https://www.theseus.fi/handle/10024/266328 (Accessed: February 16, 2023).

Turaka, S., Jagannati, V., Pappula, B., & Makgato, S. (2024). Impact of Infill Density and Morphology of Mechanical Properties of 3D Printed ABS and CF-ABS Composites using Design of Experiments. *Heliyon*, e29920. https://doi.org/10.1016/j.heliyon.2024.e29920

Winter, S., Quernheim, N., Arnemann, L., Anderl, R., & Schleich, B. (2023). Live Estimating the Carbon Footprint of Additively Manufactured Components – a Case Study. *Procedia CIRP*, 116, 642–647. https://doi.org/10.1016/j.procir.2023.02.108

Yankin, A., Alipov, Y., Temirgali, A., Serik, G., Danenova, S., Talamona, D., & Perveen, A. (2023). Optimization of Printing Parameters to Enhance Tensile Properties of ABS and Nylon Produced by Fused Filament Fabrication. *Polymers*, *15*(14), 3043. https://doi.org/10.3390/polym15143043

Zhong, H., Song, T., Li, C., Das, R., Gu, J., & Qian, M. (2023). The Gibson-Ashby model for additively manufactured metal lattice materials: Its theoretical basis, limitations and new insights from remedies. *Current Opinion in Solid State & Materials Science*, *27*(3), 101081. https://doi.org/10.1016/j.cossms.2023.101081